INTERPRETATION OF SOIL EROSION IN A POLISH LOESS AREA USING OSL, ^{137}Cs, ^{210}Pb$_{ex}$, DENDROCHRONOLOGY AND MICROMORPHOLOGY – CASE STUDY: BIEDRZYKOWICE SITE (S POLAND)

**GRZEGORZ PORĘBA[1], ZBIGNIEW ŚNIESZKO[2], PIOTR MOSKA[1],
PRZEMYSŁAW MROCZEK[3] and IRENEUSZ MALIK[4]**

[1]*Silesian University of Technology, Institute of Physics – Centre for Science and Education, Konarskiego 22B, 44-100 Gliwice, Poland*
[2]*Kazimerz Wielki University, Institute of Geography, Mińska 15, Bydgoszcz, Poland*
[3]*Maria Curie-Skłodowska University, Faculty of Earth Sciences and Spatial Management, Al. Kraśnicka 2d, 20-718 Lublin, Poland*
[4]*University of Silesia, Faculty of Earth Sciences, Będzińska 60, 41-200 Sosnowiec, Poland*

Abstract: Loess areas used for agriculture are susceptible to soil erosion. The intensive process of soil erosion in Polish loess areas began with the onset of the Neolithic and has continued intermittently until today. This work presents the results of soil erosion from simultaneous use of the ^{137}Cs and ^{210}Pb$_{ex}$ methods on an agricultural field located on loess slope. Moreover, to establish the age of accumulated sediment connected with water slope erosion, OSL dating, selected physicochemical and micromorphological analyses were applied.

The reference values of the ^{137}Cs and ^{210}Pb$_{ex}$ fallout for the studied site (Biedrzykowice, the Proszowice Plateau, Małopolska Upland) equal 2627 (45% connected with Chernobyl) and 4835 Bq·m^{-2}, respectively. The results of the ^{137}Cs and ^{210}Pb$_{ex}$ inventories measured for the agricultural field range from 730 to 7911 and from 1615 to 11136 Bq·m^{-2}, respectively. The mean soil erosion is about 2.1 kg·m^{-2}·a^{-1} (about 1.4 mm·a^{-1}). The accumulation of the colluvial sediments started in the Neolithic and drastically increased in the Middle Ages. The examined gully catchment in Biedrzykowice has probably developed quite rapidly as a result of increased erosion. This resulted in the abandonment of this area as farmland and, consequently, in the minimization of water erosion on the slope due to the entrance of woody vegetation in this area. Erosion processes were highly intensified during the last 70 years as a result of deforestation after World War II and intensive agricultural reuse of this area after a break, as indicated by isotope measurements and dendrochronology.

Keywords: Holocene soil erosion, colluvial sediment, geochronology, optical dating, micromorphology, dendrochronology.

1. INTRODUCTION

Loess areas are susceptible to soil erosion, especially when under agricultural land use. Loess areas in southern Poland have been used for agriculture since the Neolithic

(Kruk *et al.*, 1996, Kruk and Milisauskas, 1999). The advent of agriculture in this area resulted in changes of plant cover on the slopes, which increased their susceptibility to processes such as rainsplash, sheet erosion and linear erosion. Since the beginning of the Neolithic, these processes have intensified as human settlements have increased in size and number (Kruk *et al.*, 1996; Starkel, 2005). Intensification of the soil erosion processes can be noticed from the Middle Ages until the present time, but

Corresponding author: G. Poręba
e-mail: grzegorz.poreba@polsl.pl

for the last 50 years have reached their maximum (Śnieszko, 1995; Doterweich, 2008; Starkel, 2005). The accumulation of sediments at the foot of the slopes and in valley bottoms – to which the slopes episodically drain – provides a partial record of slope erosion (Śnieszko, 1991, 1995). In the case of small catchments in loess areas, soil erosion is associated rather with agricultural land use, while climate change is probably less important (Lang, 2003; Zolitschka et al., 2003; Fuchs et al., 2004; Zadorova et al., 2013).

The presence of sediments indicating both Neolithic and medieval water erosion of soil were observed as the infill relicts exposed in gully walls in the area where studies of modern soil erosion were carried out in the past (Śnieszko, 1995). The age of these colluvial sediments was documented by OSL dating. The aggradation of soil material eroded by water is synchronous with the archaeologically documented phases of agricultural colonization. The thickness of Holocene colluvial deposits accumulated in this area do not exceed 4 m. A comparison of these sediments resulting from soil erosion and characterized by limited thickness for the last 5–6 thousand years with the results of studies on the magnitude of contemporary soil erosion gives an idea of the difference in intensity of the erosion processes nowadays and in the past in this particular area (Śnieszko, 1985, 1987, 1995). One location where the impact of crop farming was significant for the natural environment in the past is near the Bronocice settlement in southern Poland. In the central part of the Nidzica Basin, one of the largest concentrations of funnel-bowl culture settlements was documented (Kruk et al., 1996). The settlement centre was located in the area of the contemporary village of Bronocice and was used by Neolithic farmers from 3900 BC to 2500 BC (Kruk et al., 2016). Numerous satellite settlements were also formed, which resulted in the water erosion of soils throughout the entire microregion (Kruk et al., 1996).

Archaeological investigation of this settlement and its neighbouring area has revealed no signs of agricultural pressure after the Neolithic until the Middle Ages, when settlements were established in locations where villages have persisted to this day (Kruk et al., 1996; Kruk and Milisauskas, 1999). Until now, only the results of radiocarbon dating of fossil soil humus lying at the base of the Holocene colluvial sediment wedge have provided a chronology for this accumulation (Kruk et al., 1996; Kruk and Milisauskas, 1999).

The precise determination of the intensity of soil erosion that occurs today, as well as from the past, is a vital problem in palaeoenvironmental studies and still requires intensive research. Moreover, the precise age of sediment formation plays an important role in modelling past environmental dynamics. Each land cover change on the slope due to ploughing produces accelerated soil erosion on the slope itself, and sediment accumulation within mid-slope flat areas and on valley floors (Zadorova et al., 2013). Reliable defining the time frame of accumulation of slope

sediments is essential to estimate the impact of the evolving agricultural systems through time. To reconstruct the age of pre-historical and historical phases of soil erosion intensification, the OSL (optically stimulated luminescence) method provides a suitable tool. Luminescence dating typically refers to the time elapsed since the last exposure of some silicate minerals to daylight. The practical usefulness of this method has been discussed for this type of sediment in the review work published by Fuchs and Lang (2009). In the case of the recent soil erosion being investigated, For studies of soil erosion which took place during the last century, two radioisotopes are very useful; the artificial radioactive fallout of ^{137}Cs (covering the period of the last 70 years) and the natural fallout of ^{210}Pb (covering the period of the last 100–150 years) have been successfully applied (Walling and He, 1999; Mabit et al., 2008). Although ^{137}Cs has been successfully used to study soil erosion, ^{210}Pb$_{ex}$ is relatively rarely used in such studies when compared to ^{137}Cs. Instead, this method is most often used to study sedimentation rates in lakes, ponds or peat environments with a time depth of about 100–150 years (Mabit et al., 2014).

The objective of this research was to use radioactive fallout, OSL and dendrochronology to further explore the potential for combining those dating methods to document soil redistribution over different time scales and human impact on the study area. In this study, we present the results of soil erosion analysis using the ^{137}Cs and ^{210}Pb$_{ex}$ methods, OSL dating, sediment analysis, micromorphology analysis and dendrochronology analysis. The soil erosion during the last 50–100 years was determined in ploughed land using both the ^{137}Cs and ^{210}Pb$_{ex}$ methods. To extend the study beyond the recent sediments to the Holocene colluvial package, luminescence dating method was also employed, specifically, the OSL dating of coarse-sized grains (Fuchs and Lang, 2009). Those dating methods, in connection with pedological and sedimentological analysis, provide information about the age of pre-historical and historical phases of intensified soil erosion. Additionally, dendrochronological analyses in our studies was used, mainly for checking whether erosion processes are currently active in the under study gully. Tree ring analyses can provide information about evolution of the gully morphology in a wide range of time from the last few decades to the hundreds of years (depending on the sampled tree age); (Vandekerckhove et al., 2001; Malik, 2008). Different types of anatomical features are used for dating erosion events in forested gullies and valley floors, these are: reaction wood, eccentric tree growth, ring reductions, and decrease of cell size after root exposure (Gärtner et al., 2001; Malik, 2006a; Stoffel et al., 2012). Those anatomical features allow, for example, to reconstruct the rate of sheet and gully erosion, or to determine the patterns of gully formation, and sometimes estimate the time when erosion started (Bodoque et al., 2005; Malik, 2006b). Considering the proposed methods and scope of research, the presented approach in

the paper allows to obtain reliable results to reconstruct the soil erosion and sediment accumulation dynamics in an area of great archaeological importance. Extensive archaeological studies show that this loess region belongs to heavily transformed loess areas under the influence of agricultural activity since the Neolithic (Kruk *et al.*, 1996).

2. MATERIALS AND METHODS

Investigated Sites

The study site is located near Biedrzykowice village (50°23'56.10"N; 20°18'44.26"E) in southern Poland, in the mesoregion named the Proszowice Plateau located on eastern part of the Małopolska Upland (Kondracki, 2002). (Figs. 1A–1D). The topographic surface of the Proszowice Plateau is situated between 220–390 m a.s.l., and the depth of the larger valleys ranges from 40 to 60 m. The mean slope inclination for a study plot is about 10°.

The oldest rocks in the exposures are chalk marbles forming culminations. Miocene gypsum and clay occur under Quaternary formations. The cover of Pleistocene glacial formations has only been studied to a very limited degree. It consists of residual clays and sands of the oldest glaciation periods, whose stratigraphic affiliation is difficult to determine. Loess deposits are the most com-

mon Pleistocene sediments. Jersak (1973) assigned these areas to the transition loess formation. Here the loess cover can reach a thickness of 20 m and colluvial sediments on the footslope and toeslope as much as 7 m. The main part of the loess cover consists of the youngest Vistulian (=Weichselian) loess deposits accumulated mainly during younger part of MIS 2, *i.e.* between 22 ka BP and 16 ka BP (e.g. Maruszczak, 1991, 2001; Jary, 2007).

Mean annual precipitation is 657 mm with the highest intensity in July. The mean value of July precipitation is 95 mm and the greatest recorded monthly precipitation (also recorded in July) was 226.1 mm (https://pl.climate-data.org/location/10413/#climate-graph). The average annual temperature is 8.2ºC, with a range from –4.4ºC (January) to 18.6ºC (July). The growing period is about 200 days of the year (Paszyński and Kluge, 1986). This area has been used as cultivated fields since the Neolithic (Kruk *et al.*, 1996, 2016; Kruk and Milisauskas, 1999). Archaeological investigations in this area suggest a strong impact by farmers on the primary landscape in the years 3900–2500 cal. BC (Kruk *et al.*, 1996, 2016). In Biedrzykowice, located almost 8 km north of the Neolithic site in Bronocice, a colluvial sediment profile preserved at the bottom of a dry valley (Sancygniówka River basin), which has been the subject of previous analyses (Śnieszko, 1985, 1995; Raven *et al.*, 1999), was selected for detailed studies.
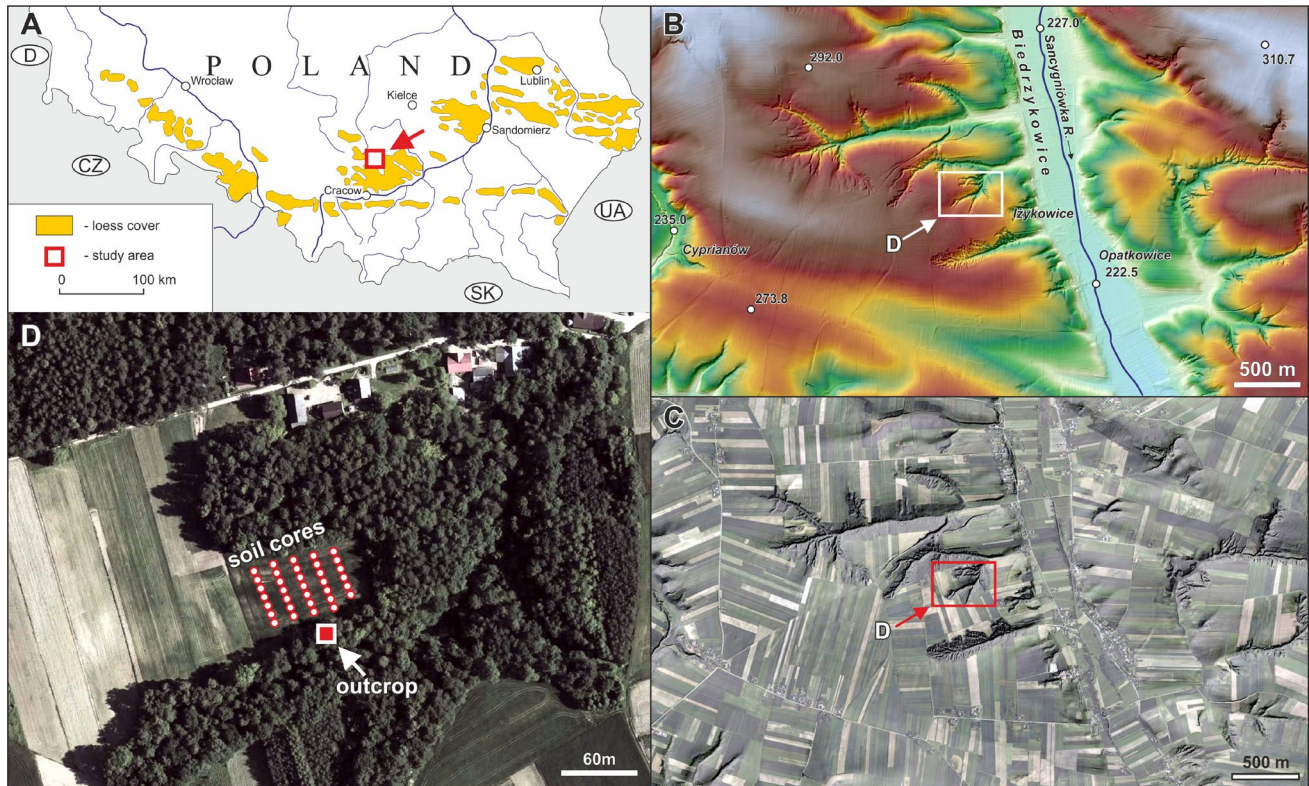

Fig. 1. A – *Location of research area on the map of loess distribution (yellow patches) in southern Poland; B – DEM model; C – orthophotomap; D – aerial photo.*

Sampling

Colluvial sediments and soil samples were collected from the wall of the gully as well as from the adjacent agricultural field (**Fig. 1D**). For the soil erosion and sedimentation study using fallout radionuclide, 34 cores were collected using a "Stiboka" motorized corer (inserting 10 cm diameter demountable steel tubes into the soil profiles) along five downslope transects from an agricultural field. The motorized sample corer allowed soil cores with a non-disturbed structure to be obtained. Core locations were recorded using an RTK GPS (Promark 220, about 0.1 m accuracy) and are presented in **Fig. 1**. The soil cores were sectioned into 10 cm intervals. Additional cores were collected from undisturbed reference sites and sectioned at 2, 3 or 5 cm increments. Reference sites were selected as places where soil erosion and sediment accumulation were not visible (mature and natural vegetation cover protects the soil surface from erosion). In the case of luminescence dating, two sets of samples were taken: the first from a gully wall and the second from an agricultural field close to the gully. We collected 13 samples for OSL dating and 50 samples for radionuclide analysis from the gully wall. The samples for optical dating were collected by using steel tubes driven into the sediment. The tubes were opened in a dark laboratory and about 1 cm of the sediment at each end was cut and removed before OSL measurement. Samples for activity measurement were taken from the surface to a depth of 500 cm. Samples for luminescence dating were also collected from three areas on the agricultural field: top of the slope, eroded area and base of the slope. This sampling was also performed using a light-protected procedure.

As well as the simultaneous application of both methods, 13 detailed micromorphological soil analyses were also carried out. The main goal of the micromorphological analyses was to determine litho- and pedological features (e.g. Kemp, 2001; Mroczek, 2008, 2013, 2018). The micromorphological samples were taken from the same horizons in the gully wall as the samples for OSL dating.

For dendrochronological analyses, we chose six larch trees (Larix decidua Mill.) growing on the edge of the gully under study. Due to erosion, the trees were tilted perpendicularly to the valley axis, and additionally their root system was partially exposed. We assumed that dendrochronological analyses would allow us to date erosion events and estimate the rate of gully hillslope retreat. Growth disturbances (tree ring reduction, tree ring eccentricity) formed after erosion events and recorded in wood of the studies trees were used to erosion dating. We collected two cores from each of the six trees with a Pressler borer at chest height, perpendicularly to the valley axis (6 cores) and parallel to the valley axis (6 cores). We also sampled by handsaw 4 exposed roots from tree number 6: root sample number 1 – sampled 5 cm from the gully edge, root sample number 2 – sampled 15 cm

from the gully edge, root sample number 3 – sampled 20 cm from the gully edge, and root sample number 4 – sampled 50 cm from the gully edge. We assumed such a strategy would allow the rate of gully hillslope retreat to be checked.

Activity measurement

Before the activity measurement, all samples were dried, placed in measurement containers and stored for a minimum of three weeks to ensure radioactive equilibrium in the decay series. The activities of ^{137}Cs and ^{210}Pb, as well as other isotopes, such as the ^{238}U series, ^{232}Th series and ^{40}K, were measured for dose rate determination by using low background high resolution gamma spectrometry analysis. The detector resolution (FWHM) was 1.8 keV and the relative efficiency was 40% at 1332 keV. The counting time was usually 80 ks and IAEA (RGU, RGTh, RGK) standards were used for calibration. The IAEA Soil-375 standard was used as a reference material for ^{137}Cs activity. The IAEA-385 standard was used to check the quality of efficiency calibration. To calculate the ^{238}U content in the sediment, the following gamma lines were taken: 295.1 keV (^{214}Pb), 352.0 keV (^{214}Pb), 609.3 keV (^{214}Bi) and 1120.3 keV (^{214}Bi). For the ^{232}Th decay chain, the following gamma lines were considered: 583.0 keV (^{208}Tl), 911.2 keV (^{228}Ac) and 2614.4 keV (^{208}Tl). To calculate the ^{40}K content, the 1460.8 keV gamma line was taken. To calculate the ^{137}Cs content, the 661.7 keV gamma line was used. The total activity of ^{210}Pb in the samples was measured at 46.5 keV and the concentration of the supported ^{210}Pb was assayed by measuring the short-lived daughters of ^{226}Ra. The unsupported ^{210}Pb activity (^{210}Pb$_{ex}$) in the samples was calculated by subtracting the supported ^{210}Pb from the total concentration of ^{210}Pb. In the case of ^{210}Pb, the results were corrected for self-absorption, in accordance with Cutshall et al. (1983).

Dose rate calculation

The measured activities of radioisotopes in the sediment and soil samples were converted into dose rates by using the conversion factors described by Guerin et al. (2011). The dry dose rates (Adamiec and Aitken, 1998; Guerin et al., 2011) were adjusted for water content, following Aitken (1985). The water content of samples measured in the laboratory was no higher than 15%, so we used a value of $10 \pm 5\%$ for our calculations (Bluszcz, 2000). The cosmic ray dose-rate at the site follows the calculations suggested by Prescott and Hutton (1994).

The results of radionuclide analysis as results of dose rate calculation are summarized in **Table 1**. For the sediment samples, the dating of the ^{137}Cs activity was included in the calculation of the dose rate, according to the procedure described in (Moska et al., 2004; Poręba et al., 2006).

Table 1. *Results of activity concentration measurement (based on low-level semiconductor γ-spectrometry), dose rate calculation, D_e estimation and OSL ages for sediment samples from Biedrzykowice.* [1]*Doses for samples collected from a depth lower than 50 cm were corrected with respect to range of gamma rays.* [2]*Dose rates in this column were obtained by using portable gamma spectrometer in situ.*

Sample name	Lab code	Depth (cm)	U (Bq·kg⁻¹)	Th (Bq·kg⁻¹)	K (Bq·kg⁻¹)	Dose rate (Gy·ka⁻¹)	Dose rate[2] (Gy·ka⁻¹)	Palaeodose (Gy)	OSL age (ka)
Bie_1_1	GdTL-2906	11–15	31.84±0.44	39.09±0.78	508±17	2.84±0.21[1]	2.74±0.20	1.831±0.037	0.645±0.049
Bie_1_2	GdTL-2907	26–30	34.21±0.36	40.08±0.62	502±16	3.08±0.21[1]	3.03±0.22	2.182±0.085	0.708±0.056
Bie_1_3	GdTL-2908	55–59	32.71±0.39	38.35±0.65	527±17	3.07±0.22	3.04±0.23	2.29±0.14	0.746±0.070
Bie_1_4	GdTL-2909	120–124	29.53±0.55	36.80±0.83	492±17	2.85±0.20	3.12±0.23	1.922±0.031	0.674±0.049
Bie_1_5	GdTL-2910	151–155	30.82±0.36	38.15±0.63	559±18	3.09±0.22	2.94±0.22	3.052±0.068	0.988±0.074
Bie_1_6	GdTL-2911	200–204	30.23±0.23	38.55±0.48	539±16	3.01±0.22	3.01±0.23	7.88±0.20	2.62±0.20
Bie_1_7	GdTL-2912	231–235	30.11±0.39	37.68±0.69	532±17	2.96±0.21	2.96±0.23	11.11±0.14	3.75±0.27
Bie_1_8	GdTL-2913	286–290	27.97±0.39	34.45±0.68	533±17	2.86±0.21	3.12±0.24	16.32±0.28	5.71±0.43
Bie_1_9	GdTL-2914	356–360	31.51±0.42	34.57±0.70	532±17	2.92±0.21	3.03±0.23	17.67±0.28	6.05±0.45
Bie_1_10	GdTL-2915	380–384	26.20±0.45	31.80±0.74	510±17	2.70±0.20	2.54±0.20	19.70±0.15	7.30±0.54
Bie_1_11	GdTL-2916	406–410	30.63±0.48	34.93±0.77	534±18	2.90±0.21	2.72±0.21	26.19±0.23	9.03±0.66
Bie_1_12	GdTL-2917	425–429	32.62±0.48	36.65±0.79	524±18	2.94±0.21	2.98±0.23	32.40±0.40	11.02±0.80
Bie_1_13	GdTL-2918	471–475	35.15±0.29	40.70±0.53	483±15	2.93±0.21	2.93±0.23	35.8±1.0	12.22±0.94
Bie_2_1	GdTL-3067	12–15	29.99±0.73	34.01±0.81	504±21	2.89±0.22[1]	-	2.25±0.18	0.779±0.086
Bie_2_2	GdTL-3068	52–57	30.08±0.72	32.46±0.76	508±21	3.01±0.22	-	42.1±0.95	14.0±1.0
Bie_3_1	GdTL-3069	12–15	31.01±0.67	29.98±0.63	502±21	2.80±0.21[1]	-	3.97±0.30	1.42±0.15
Bie_3_2	GdTL-3070	52–57	24.94±0.65	27.26±0.72	455±19	2.64±0.19	-	44.52±0.68	16.9±1.2
Bie_4_1	GdTL-3071	14–18	32.61±0.79	34.72±0.83	528±22	3.02±0.23[1]	-	0.528±0.033	0.175±0.017
Bie_4_2	GdTL-3072	54–57	31.76±0.76	32.62±0.82	519±22	3.08±0.22	-	2.58±0.18	0.838±0.084
Bie_4_3	GdTL-3073	91–95	30.28±0.64	33.10±0.67	545±22	3.11±0.23	-	13.05±0.31	4.20±0.33
Bie_4_4	GdTL-3074	110–114	30.26±0.75	33.84±0.84	558±24	3.16±0.23	-	19.83±0.61	6.28±0.50
Bie_4_5	GdTL-3075	145–149	28.03±0.95	33.18±0.94	595±23	3.19±0.24	-	39.17±0.83	12.28±0.96

[137]Cs and ^{210}Pb dating

Caesium-137 (half-life 30.1 years) is a radioisotope whose main source in the environment is above-ground nuclear weapon tests in the 1950s and 1960s. The ^{137}Cs fallout connected with nuclear weapon testing is known as global fallout, and its distribution depends on latitude and precipitation. The highest intensity of ^{137}Cs deposition occurred in the period 1961–1963. Additionally, another ^{137}Cs fallout connected with the Chernobyl accident of 1986 has taken place in Europe. [137]Cs is strongly adsorbed into soil particles (Ritchie and McHenry, 1990) after its deposition on the ground surface, In areas contaminated as a result of the Chernobyl accident, calculation of soil erosion based on the ^{137}Cs inventories can be difficult due to problems in distinguishing between global and Chernobyl ^{137}Cs fallouts (Golosov *et al.*, 1999; Poręba and Bluszcz, 2007). In contrast to ^{137}Cs, [210]Pb (with a half-life of 22.2 years) is a natural radioactive isotope which is a part of the [238]U decay chain. This isotope is derived from the radioactive decay of [222]Rn, a daughter of [226]Ra. [210]Pb produced from [226]Ra in situ in soil is known as supported, whereas the ^{210}Pb originating from atmospheric fallout is named unsupported (or [210]Pb$_{ex}$), and is used widely to study the accumulation rates of various sediments. The activity of [210]Pb$_{ex}$ is usually calculated by subtracting the supported ^{210}Pb established via the activity of the [226]Ra daughters from the total ^{210}Pb in a given soil or sediment sample (Walling, 1998; Walling and He, 1999; Mabit *et al.*, 2014).

The measured ^{137}Cs and [210]Pb$_{ex}$ activities were converted to inventories according to the formula described by Sutherland (1992) and are presented in **Figs. 2–3**. The simple comparison between the measured values of the ^{137}Cs or [210]Pb$_{ex}$ inventories and the reference inventory values of ^{137}Cs or [210]Pb$_{ex}$ allows us to recognize erosion and deposition areas; however, to obtain quantitative estimates of soil erosion, one of several available models must be used (Walling and Quine, 1990; Walling and He, 1999).To estimate soil erosion based on ^{137}Cs and [210]Pb$_{ex}$, the proportional model (^{137}Cs) as well as two mass balance models (^{137}Cs, [210]Pb$_{ex}$) were applied (Walling and Quine, 1990; Walling and He, 1999; Poręba, 2006). The equation for the proportional model can be written as (Walling and Quine, 1990):

$$Y = \frac{BdX}{10TP} \qquad (2.1)$$

where:
- Y – mean annual soil loss (t·ha⁻¹·a⁻¹),
- B – bulk density of the soil (kg·m⁻³),
- d – depth of the plough layer (m),
- X – percentage reduction in total ^{137}Cs inventory (defined as $(A_{ref} - A)/A_{ref} \cdot 100$),
- A_{ref} – local ^{137}Cs reference inventory (Bq·m⁻²),
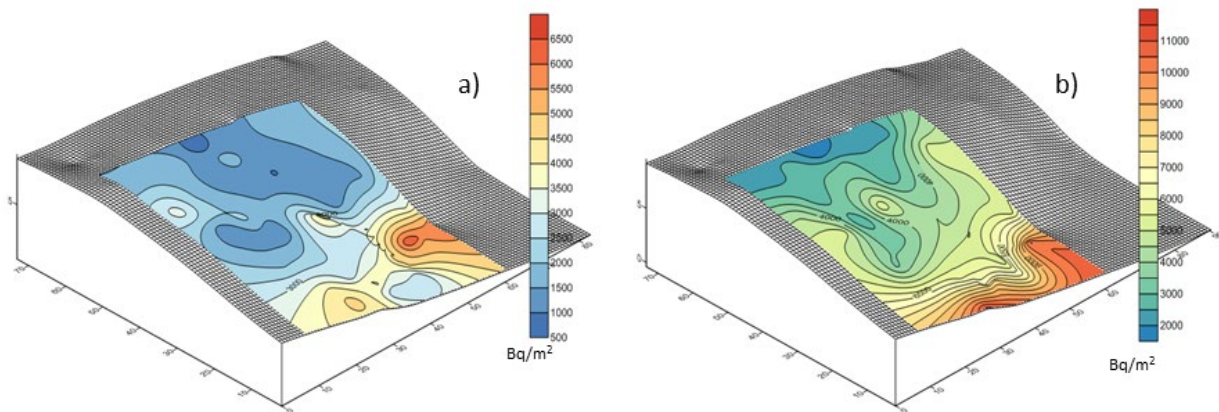- A – measured ^{137}Cs inventory at the sampling point (Bq·m⁻²),

Fig. 2. *The spatial patterns of ^{137}Cs and ^{210}Pb$_{ex}$ inventories on the studied agricultural field. The data on the figure are expressed in Bq·m^{-2}.*

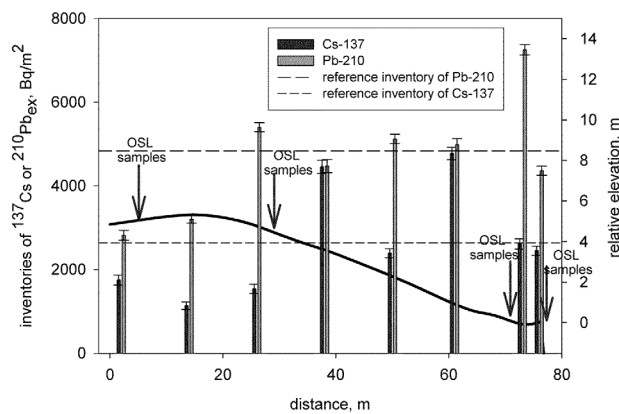**Fig. 3.** *The downslope change of ^{137}Cs and ^{210}Pb$_{ex}$ inventories. On the figure is marked the shape of the slope.*

- T – time elapsed since initiation of ^{137}Cs accumulation (a),
- P – the particle size correction factor (possible difference between the grain size composition of the mobilized sediment and the original soil). The value of this factor could be calculated according to He and Walling (1996).

The main assumption for the proportional model is that ^{137}Cs is completely mixed within the plough layer. If this is true, then the soil loss is directly proportional to the ^{137}Cs loss from the soil profile. Although this model is relatively easy to use, it has several limitations. For instance, this model assumes that caesium is uniformly distributed in the plough layer. Immediately after fallout, the surface contained more caesium than the underlying soil horizons due to agricultural mixing, e.g. ploughing.

This could result in an overestimation of soil loss (Walling and Quine, 1990). Two kinds of mass balance models were also used to calculate soil erosion and deposition. The first mass balance model was described by Zhang *et al.* (1990) and is referred to as the simplified mass balance model. The main assumption of this model is that the total ^{137}Cs fallout occurred in 1963. The mean annual soil loss rate can be expressed as follows:

$$Y = 10dB\left[1 - \left(1 - \frac{X}{100}\right)^{1/(t-1963)}\right] \qquad (2.2)$$

where:
- Y – mean annual soil loss (t·ha^{-1}·yr^{-1}),
- d – depth of the plough layer (m),
- B – bulk density of soil (kg·m^{-3}),
- X – the percentage reduction in total ^{137}Cs inventory (defined as (Aref – A)/Aref ·100),
- t – time since the year 1963.

Although this model is very easy to use, the main assumption of this approach that the total ^{137}Cs fallout input occurred in 1963 seems to be an oversimplification. This model does not take into account the value of ^{137}Cs freshly removed from the soil surface before incorporation into the plough layer by ploughing. The problem with selective sorption of ^{137}Cs by soil particles could be solved by adding a particle size correction factor (Zhang *et al.*, 1999). Another problem with the simplified mass balance model is the assumption of the ^{137}Cs fallout in 1963. This does not take into account areas contaminated by Chernobyl caesium, such as the study area.

To overcome the problem with selective sorption, and also removing the fresh deposition of ^{137}Cs before mixing by ploughing, the mass balance model was improved by He and Walling (1997). This model was also used to calculate soil erosion based on the ^{210}Pb$_{ex}$ inventories.

According to He and Walling (1997), this model could be written as follows:

$$\frac{dA(t)}{dt} = (1 - \Gamma)I(t) - \left(\lambda + P\frac{R}{d}\right)A(t) \qquad (2.3)$$

where:
- $A(t)$ – cumulative ^{137}Cs or $^{210}Pb_{ex}$ activity per unit area ($Bq \cdot m^{-2}$),
- R – soil erosion rate ($kg \cdot m^{-2} \cdot a^{-1}$),
- d – the average plough depth ($kg \cdot m^{-2}$),
- λ – the radioactive decay constant for ^{137}Cs or $^{210}Pb_{ex}$ (a^{-1}),
- $I(t)$ – annual ^{137}Cs or $^{210}Pb_{ex}$ deposition flux ($Bq \cdot m^{-2}\ a^{-1}$),
- Γ – the percent of the fresh deposition of ^{137}Cs or $^{210}Pb_{ex}$ removed by erosion before mixing into the plough layer,
- P – the particle size correction factor (see footnotes for **Eq. 2.1**)

For the areas where deposition of soil occurs, the mass balance model could be written according to Walling and He (1999) to calculate the soil deposition rate:

$$R' = \frac{A_{ex}}{\int_{t_0}^{t} C_d(t')e^{-\lambda(t-t')}dt'} \qquad (2.4)$$

where:
- A_{ex} – is the excess ^{137}Cs or $^{210}Pb_{ex}$ inventory ($Bq \cdot m^{-2}$) / total measured inventory minus reference value of inventory/,
- $C_d(t')$ – is a concentration of deposited sediment which is a sum of activities of mobilized sediment from upper part of the slope.

Luminescence dating

Samples for OSL dating were treated with 10% HCl and 10% H_2O_2 for 48 hours to remove carbonates and organic material, respectively. Quartz was extracted from the 90–125 µm grain fraction by using density separation (sodium polytungstate). Finally, quartz grains were etched using 40% HF to remove their outer layer (Aitken, 1985, 1998). After etching, they were washed in HCl (20%) to remove any precipitated fluorides. The grains were then mounted on stainless steel discs using silicone oil. All treatment was conducted under subdued red light.

Quartz from each sample was checked for purity by means of an IR-test. No samples showed a significant IRSL signal, *i.e.* the natural and regenerated signal ratios of the IRSL to the blue-light stimulated luminescence were ≤ 5%. The SAR procedure which was used for equivalent dose determination did not contain IRSL step.

Optically stimulated luminescence measurements (OSL) were made using an automated Daybreak 2200 TL/OSL reader (Bortolot, 2000), equipped with a calibrated $^{90}Sr/^{90}Y$ beta source (dose rate of $2.95 \pm 0.09\ Gy \cdot min^{-1}$).

The determination of equivalent doses of quartz grains was performed using multi-grain aliquots, each containing *ca.* 1 mg of quartz grains. A 6 mm mask was used to disk preparation, it means that on the single disk should be about 1500 quartz grains with 90–125 µm diameter (Herr *et al.*, 2012). For stimulation, blue diodes (470 ± 4 nm) delivering 45 mW·cm^{-2} at the sample position were used. Equivalent doses were determined using a single-aliquot regenerative-dose (SAR) protocol (Murray and Wintle, 2000). Dose recovery and thermal transfer tests were performed for each sample and a preheat plateau test was performed to establish the most appropriate preheat temperature.

Micromorphological analyses

Micromorphological analyses were carried out on a selected sequence of colluvial sediments with intercalated palaeosoil horizons in the gully (**Figs. 4–5**). The micromorphological samples were taken from the same horizons in the vertical outcrop as the samples for OSL dating. The material was collected in Kubiena tins (8×6×4 cm) directly from selected colluvial layers and soil horizons. Thin sections were made of samples according to the methodology proposed by Lee and Kemp (1992) and modified by Mroczek (2008). The size of the individual thin sections was ~8×6 cm, and their thickness ranged from 20 to 30 µm. Thin sections were observed using a polarizing microscope with magnifications up to 200×.

Dendrochronology

Within cores we dated the eccentric growth of trees, which is formed due to trees tilting and is relatively easy to observe in the wood cross-sections (**Fig. 6A**). We used cores collected perpendicularly to the gully axis for eccentric growth analyses. After root exposure, a tree produces reduced rings, therefore we also analysed ring reduction in the sample cores (**Fig. 6B**). The eccentric growth of trees develops on the side in which the tree stem is tilted (in the case of conifers), while ring reduction occurs on the entire perimeter of the tree. Every core was glued to wooden holders and dried. Next, the cores and root samples were sanded by 200, 500, and 1000 sand paper to better reveal the ring structure. We measured the ring width in the collected cores using the LINTAB measuring system, and visually cross-dated ring series from individual trees. Eccentric growth was calculated using a formula proposed by Wistuba *et al.* (2013). Based on previous studies, we presumed that the yearly variation of the eccentricity index should be more than 50% for dating mass-movements or erosion (Malik and Wistuba, 2012). We used cores collected parallel to the gully axis for ring reduction analyses. For ring reduction calculation, we modified the method proposed by Schwiengruber *et al.* (1985). We assumed that reduction occurs when at least 3 successive rings are reduced by more than 75% in relation to the average ring width in an individual core.
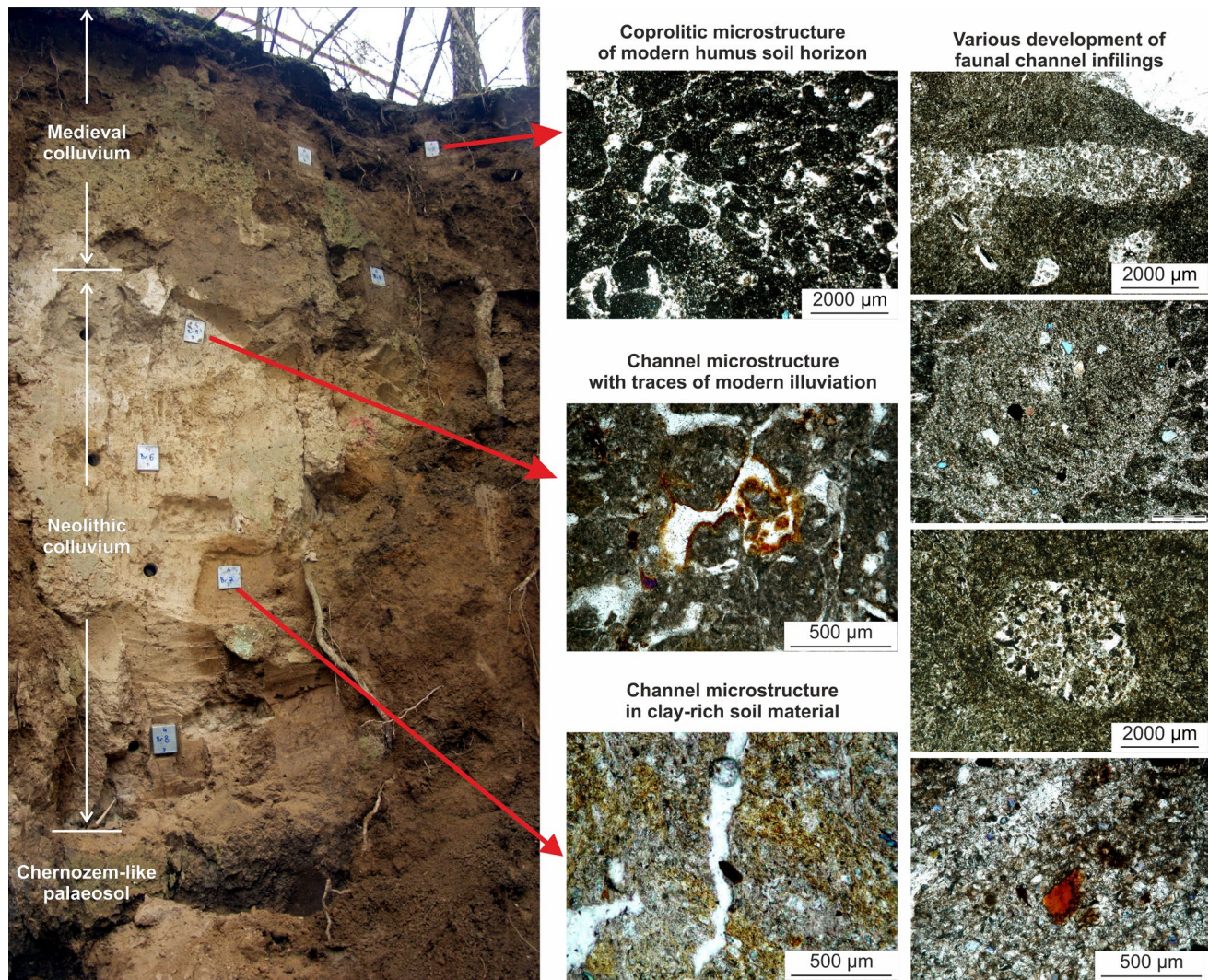
Fig. 4. *Micromorphological features and genetic interpretation of upper part of soil-colluvial sequence in Biedrzykowice.*

Grain size distribution measurements

Grain-size distributions were determined using a Malvern Mastersizer 3000 laser diffractometer. Before measurement, organic matter was removed by H_2O_2. The samples were dispersed with sodium hexametaphosphate and shaken overnight in distilled water to disperse (Mason *et al.*, 2003; Schaetzl *et al.*, 2014).

3. RESEARCH RESULTS

Measured ^{137}Cs and ^{210}Pb$_{ex}$ activities

The ^{137}Cs and ^{210}Pb$_{ex}$ inventories measured for the soil cores from the agricultural field range from 730 to 7911 Bq·m^{-2} and from 1615 to 11136 Bq·m^{-2}, respectively (**Figs. 2–3**). To calculate the rate of soil erosion and sediment accumulation, the reference inventories of ^{137}Cs and ^{210}Pb$_{ex}$ need to be known. The reference inventories for ^{137}Cs and ^{210}Pb$_{ex}$ were measured in undisturbed soil cores collected from the area surrounding the study field. **Fig. 7** provides an example of the depth distributions of ^{137}Cs and ^{210}Pb$_{ex}$ at the reference site. ^{137}Cs was found at a depth of about 25–30 cm and, simultaneously, ^{210}Pb$_{ex}$ was found at a similar depth. Both depth distributions show an exponential decrease with depth, however, the maximum ^{137}Cs concentration was just below the surface. This behaviour of caesium in soil has also been described by Li *et al.* (2009). Based on the reference cores, the reference inventories were estimated. The mean value of the total baseline inventory of ^{137}Cs for the study area is 2627 Bq·m^{-2}. This value is substantially higher than the mean value for Poland (Pietrzak-Flis, 2000; Strzelecki *et al.*, 1994). This is because the study area is located in the region where larger ^{137}Cs concentrations in soil are expected due to the Chernobyl accident. The values of Chernobyl ^{137}Cs depend on the trajectories of the main radioactivity clouds, and on the precipitation in the area of interest at the time of the accident (Stach, 1996;

Fig. 5. *Micromorphological characteristic of lower part of soil-colluvial sequence in Biedrzykowice. The microphotograph presents massive microstructure in clay-rich soil material.*

Fig. 7. *The example of depth distributions of ^{137}Cs and ^{210}Pb$_{ex}$ for a reference site.*

Strzelecki *et al.*, 1994). Increased values of Chernobyl ^{137}Cs concentration are found along the line of Warsaw – Opole – the Kłodzko Basin. The largest values of Chernobyl ^{137}Cs fallout were found in the Opole and Silesia regions (SW Poland), and in the Kłodzko Basin in the foreland of the Sudetes Mountains. In these areas, the values of Chernobyl ^{137}Cs concentration were between 15.6 kBq·m^{-2} and 19.3 kBq·m^{-2}, with the maximum value of 96 kBq·m^{-2} in the Nysa area (Stach, 1996; Strzelecki *et al.*, 1992, 1994; Szewczyk, 1994). The strong spatial
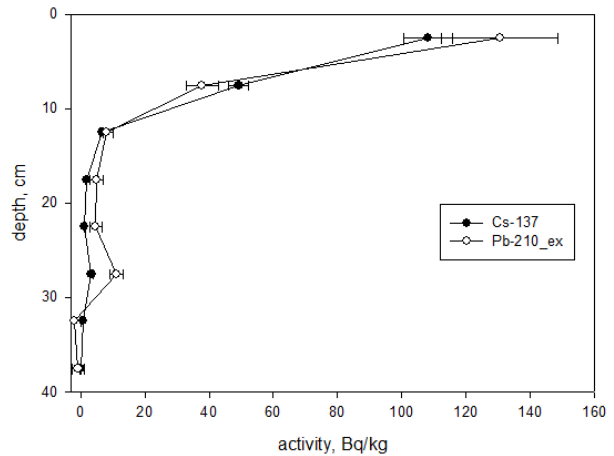
variability of the ^{137}Cs concentration from the Chernobyl accident makes it difficult to use ^{137}Cs in soil erosion studies (Golosow *et al.*, 1999). The mean value of the ^{137}Cs deposition for the Świętokrzyskie region is 1.28 kBq·m^{-2}, and the range is from 0.31 to 3.55 kBq·m^{-2} (Issajenko *et al.*, 2014). Unfortunately, the authors of that study collected only the top 10 cm of soil, thus this value could be systematically lower than in our case. The mean value of ^{137}Cs deposition for Poland is 1.53 kBq·m^{-2}, and the range is from 0.22 to 17.79 kBq·m^{-2} (Issajenko *et al.*, 2014).

The calculated ^{137}Cs reference inventory, based on latitude and mean annual precipitation for the study area, is 1269 Bq·m^{-2}. To use a more sophisticated model to calculate soil erosion based on the ^{137}Cs inventories, knowledge of the annual fallout of ^{137}Cs is needed. Unfortunately, the approach described above does not provide this information. There are few places in the world where the deposition of ^{137}Cs has been measured since nuclear weapon tests started, and the information about the rate of fallout is essential to use ^{137}Cs to study soil erosion. In Poland, the deposition of ^{137}Cs has been measured since 1970 (Stach, 1996). The concentration of
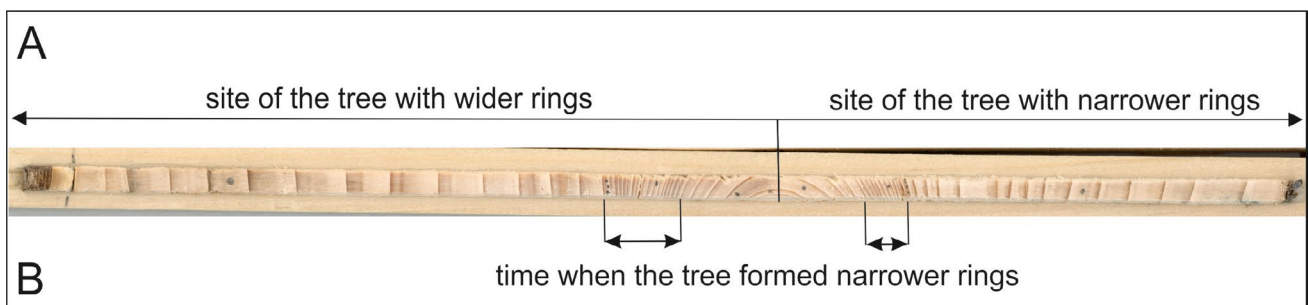

Fig. 6. *Core with eccentric growth of tree (A), and ring reduction (B)*

Chernobyl ^{137}Cs varies widely even within one field (Dubois and Bossew, 2003; Strzelecki *et al.*, 1992, 1994; Szewczyk, 1994). The percentage of the Chernobyl deposition in the global deposition of ^{137}Cs must be known to be able to use the models to calculate soil erosion from the ^{137}Cs activity data. Nowadays, there is a problem with separating the Chernobyl fallout from global ^{137}Cs fallout. A valuable tracer of the Chernobyl fallout was another caesium isotope [134]Cs, but this isotope has a relatively short half-life (approx. 2 yr) and is no longer present in the environment. The annual fallout of ^{137}Cs could be obtained according to calculations proposed by Walling and He (1999), but this approach seems to be an oversimplification due to changes in the ^{137}Cs fallout in the past and local rainfall distribution. In the present study, the reference inventory of the ^{137}Cs fallout was separated from the Chernobyl fallout and from the global weapon test fallout by estimating the baseline inventory from atmospheric records. Moreover, this method is useful to obtain information about the variability of the ^{137}Cs deposition during the period of the fallout accumulation (Lu and Higgitt, 2000; Poręba and Bluszcz, 2007). This method allows us to estimate an initial inventory of ^{137}Cs connected with nuclear weapon tests, based on the precipitation data (IMGW-PIB data - Institute of Meteorology and Water Management - National Research Institute) and data provided by Sarmiento and Gwinn (1986) (Poręba and Bluszcz, 2007). The global ^{137}Cs fallout calculated by this model is 1456 Bq·m^{-2} (**Fig. 8a**). This value is connected with nuclear weapon tests and is also called the global caesium fallout. The difference between this value and the value of caesium fallout measured at the reference site is associated with the Chernobyl fallout. For the study area, about 45% of the total caesium fallout is connected with the Chernobyl accident.

The ^{137}Cs fallout calculations for the study area are presented in **Fig. 8b**. For the study area, about 44% of the global caesium fallout occurred in the period 1962–1964.

These calculations take into account both the nature of rainfall and seasonal variations in rainfall over the period of fallout.

The mean value for the [210]Pb$_{ex}$ reference inventories is 4835 Bq·m^{-2}. This value was obtained from the measurement of reference soil cores and is similar to values obtained by other authors (Porto *et al.*, 2006; Kato *et al.*, 2010). In this case, [210]Pb$_{ex}$ constant deposition flux was assumed and the annual fallout of ^{210}Pb for the study area was estimated to be 150 Bq·m^{-2}·a^{-1}. Compared to ^{137}Cs, which is frequently used to study soil erosion, [210]Pb$_{ex}$ is rarely used for this purpose. [210]Pb$_{ex}$ is mainly used to study the sedimentation rate of lake sediments or peat accumulation. Nowadays, knowledge concerning the global values of [210]Pb$_{ex}$ is also limited (Baskaran, 2011; Mabit *et al.*, 2014) and the range of the [210]Pb$_{ex}$ fallout is relatively large.

Based on the reference values of ^{137}Cs, about 62% of the study area was defined as eroding while, based on the [210]Pb$_{ex}$ inventories, this figure was about 50%. The simple comparison between the measured value of the ^{137}Cs or [210]Pb$_{ex}$ inventories and the value of the reference inventory of ^{137}Cs or [210]Pb$_{ex}$ allows us to recognize erosion and deposition areas; however, to obtain quantitative estimates of soil erosion, one of several available models must be used (Walling and Quine, 1990). To estimate soil erosion based on ^{137}Cs and [210]Pb$_{ex}$, the proportional model (^{137}Cs) as well as mass balance models (^{137}Cs, [210]Pb$_{ex}$) were applied (Walling and Quine, 1990; Walling and He, 1999; Poręba, 2006). The results of calculations for soil erosion for the valley section in question, using the four models, are presented in **Fig. 9**. The calculated soil erosion for the studied area shows significant variation. In the case of the ^{137}Cs measurement and the proportional model, the obtained soil loss results vary from 0.49 to 3.99 kg·m^{-2}·a^{-1}, whereas in the case of the simplified mass balance model the range is from 0.61 to 7.89 kg·m^{-2}·a^{-1}. The soil erosion rates calculated by the
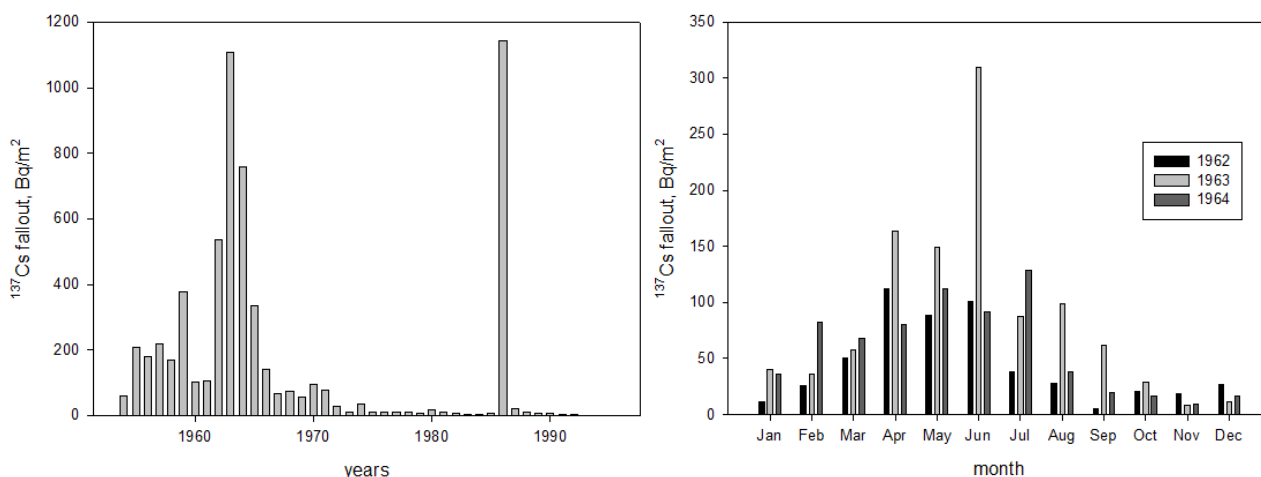

Fig. 8. a) *The calculated annual* [137]*Cs inventories based on precipitation data and model Sarmiento-Gwinn for a study site; b) The calculated monthly* [137]*Cs inventories based on precipitation data and model Sarmiento-Gwinn for a study site for the period 1962–1964.*
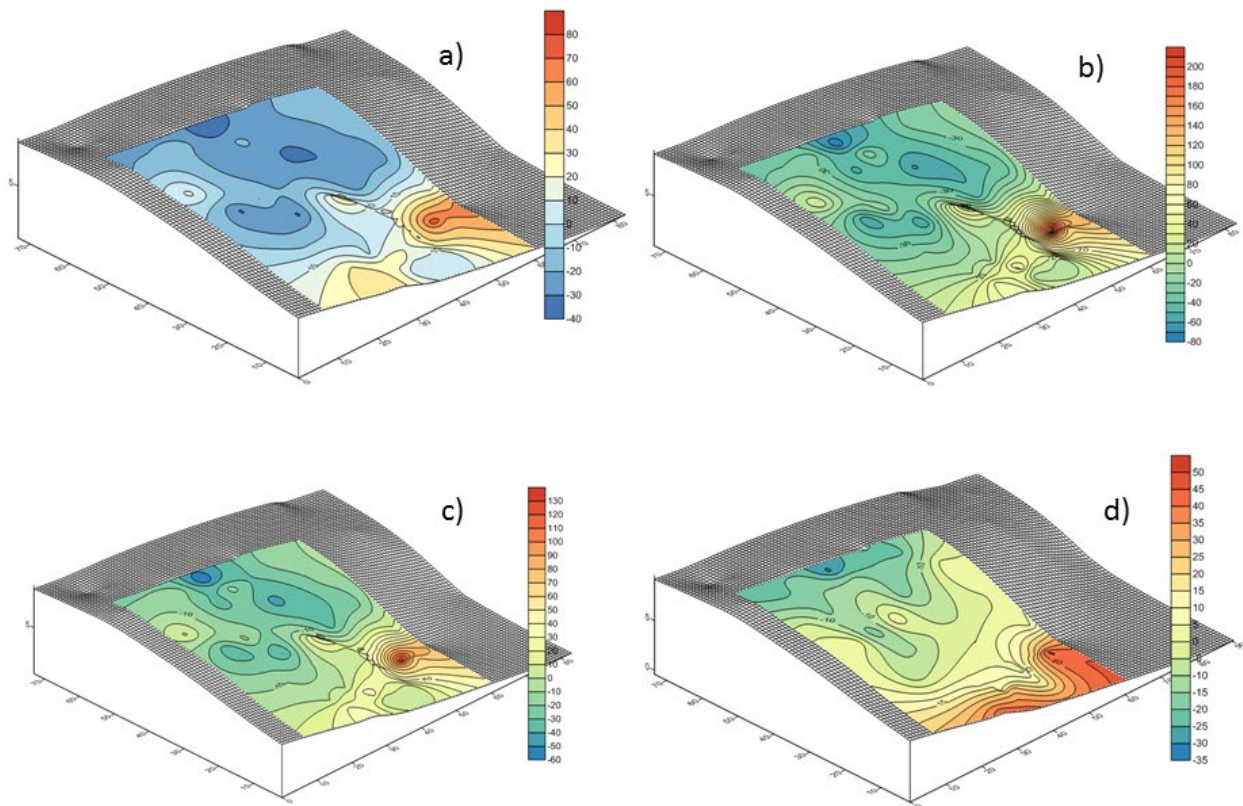
Fig. 9. *The spatial patterns soil erosion and sediment accumulation calculated by different models based on radionuclide inventories on the studied agricultural field: a) proportional model based on* [137]*Cs inventories, b) simplified mass balance model based on* [137]*Cs inventories, c) improved mass balance model based on* [137]*Cs inventories, d) improved mass balance model based on* [210]*Pb$_{ex}$ inventories.*

improved mass balance model for the cultivated slopes vary from 0.35 kg·m^{-2}·a^{-1} to 5.98 kg·m^{-2}·a^{-1}. The mean soil erosion rate calculated for the proportional model is 2.09 kg·m^{-2}·a^{-1}, the mean soil erosion rate for the simplified mass balance model is 3.35 kg·m^{-2}·a^{-1}, with 2.18 kg·m^{-2}·a^{-1} in the case of the improved mass balance model. The results obtained by the proportional model and improved mass balance model are similar, while the results of soil erosion loss obtained using the simplified mass balance model are substantially higher. The simplified mass balance model assumes that the entire caesium fallout occurred in one year, which might be a source of error in the case of areas contaminated by the Chernobyl caesium fallout. In the case of the improved mass balance model, the monthly (or at least annual) values of caesium fallout, as well as the initial distribution of fresh fallout of caesium in the top soil, are considered. Still, the improved mass balance model probably provides the most reliable results, but requires several additional parameters (Walling and He, 1999; Poręba and Bluszcz, 2008).

The soil erosion estimation based on the [210]Pb$_{ex}$ measurements and the improved mass balance model ranged from 0.22 kg·m^{-2}·a^{-1} to 3.07 kg·m^{-2}·a^{-1}, with a mean value of 1.38 kg·m^{-2}·a^{-1}.The range of calculated soil

erosion is similar to that obtained by the proportional model or improved mass balance model in the case of caesium measurement, but the mean value of soil erosion is slightly smaller than the values obtained in those latter cases. That difference can be attributed to different periods covered by measurements of caesium and lead. The results suggest an intensification of soil erosion after 1950. The change in land use is also supported by a different distribution of the intensity of the erosion and accumulation processes within the examined slope. In the case of ^{137}Cs, large soil erosion values were obtained in the middle part, but in the upper part of the slope for [210]Pb$_{ex}$. However, the accumulation in the case of the [210]Pb$_{ex}$ isotope analysis is greatest for the zone just above the edge of the gully (mean value 26 cm during 100 years) while the greatest accumulation for the ^{137}Cs isotope measurement is approximately 10–15 m from the edge of the ravine (mean value 25 cm during 54 years). This may be the result of changes in land use after World War II. As a result of intensive mechanical cultivation, the slope has been remodelled.

It is quite clear that the soil erosion rate calculated on the basis of radioisotope data depends on the model used; still we can note that the proportional model and the im-

proved mass balance model provide similar results. Similar discrepancies between the results obtained by different models are also present when calculating sediment accumulation. In this case, the results using the proportional model and the improved mass balance model are also similar, whereas those of sediment accumulation obtained using the simplified mass balance model are slightly higher. Surprisingly, sediment accumulation at the foot of the slope for two sampling points by ^{137}Cs measurements was close to zero, which suggests no sediment delivery to those locations. This is also confirmed by the depth distribution of isotopes in the sediment profiles.

Results of OSL dating

OSL samples from four locations within the study area were analysed: one sampling location at the top of the slope, one located in the eroded part of the slope, one at the foot of the slope and one from the wall of a gully located at the foot of the studied slope. The locations of sampling points for luminescence dating on the slope are marked in **Fig. 3**. **Figs. 10–13** present the results of OSL

dating for soil samples collected from the sampling positions on the slope (**Figs. 10B–12B**), as well as the samples collected from the gully wall (**Fig. 13B**). The results of OSL dating for the Biedrzykowice study site are also given in **Table 1**. This table also presents the results of radionuclide analysis in the dated samples, dose rate calculations and doses. To determine OSL ages, the central age model (CAM) proposed by Galbraith *et al.* (1999) was used.

In the case of ploughed land, the luminescence ages of the deeper layer (loess) are between 14–17 ka (Bie_2_2 and Bie_3_2; GdTL-3068, GdTL-3070; **Table 1**). The OSL distributions are almost symmetric, thus the results from CAM model probably represent the true depositional age. The luminescence ages of the layers closer to the soil surface are between 0.779–1.42 ka (Bie_2_1 and Bie_3_1; GdTL-3067, GdTL-3069), and OSL age distributions are positively skewed and asymmetric. Those distributions could be a result of incomplete bleaching or post depositional processes, particularly as in this case we are dealing with both biological and mechanical mixing (in the form of the incorporation of
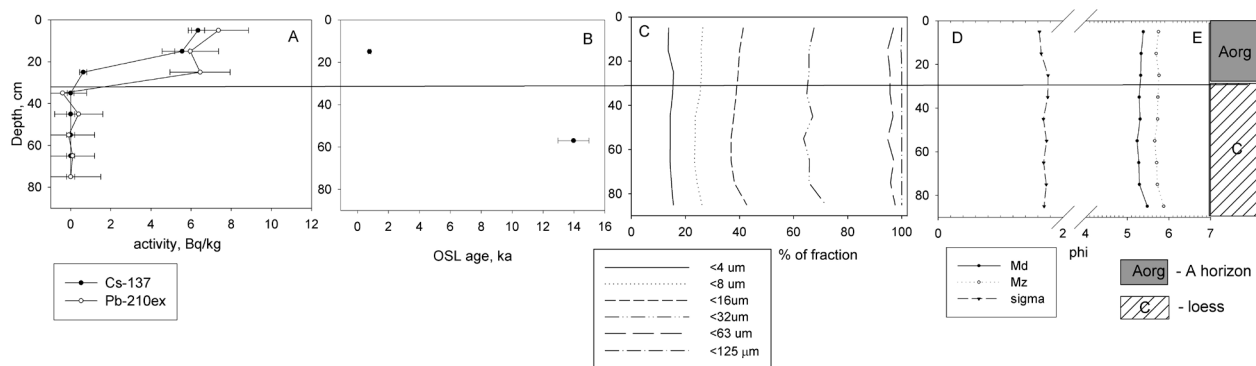

Fig. 10. *The depth distribution of the ^{137}Cs and [210]Pb$_{ex}$ (A), SAR OSL ages (B), grain size composition (C, D) and stratigraphy (E) for the soil core collected from the upper part of the slope.*

Fig. 11. *The depth distribution of the ^{137}Cs and [210]Pb$_{ex}$ (A), SAR OSL ages (B), grain size composition (C, D) and stratigraphy (E) for the soil core collected from the middle part of the slope.*

Fig. 12. *The depth distribution of the ^{137}Cs and ^{210}Pb$_{ex}$ (A), SAR OSL ages (B), grain size composition (C, D) and stratigraphy (E), for the soil core collected from the lower part of the slope.*
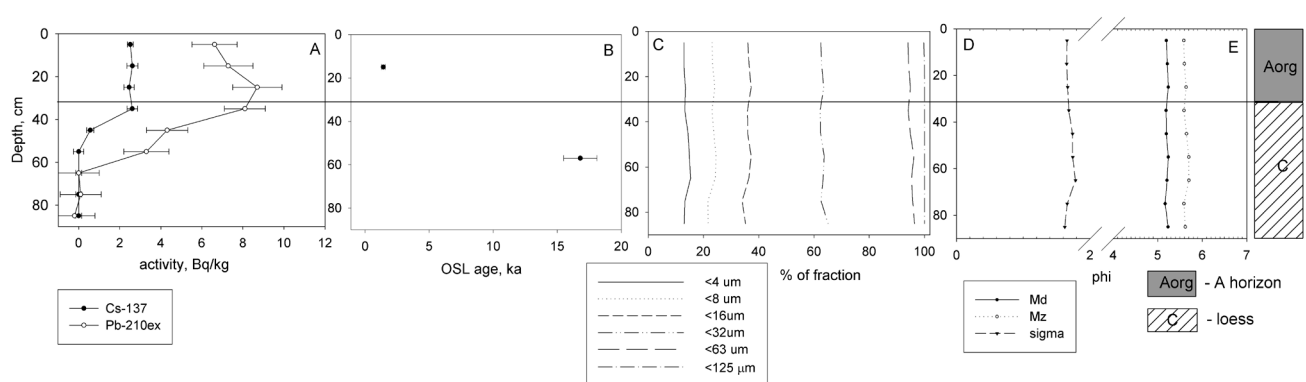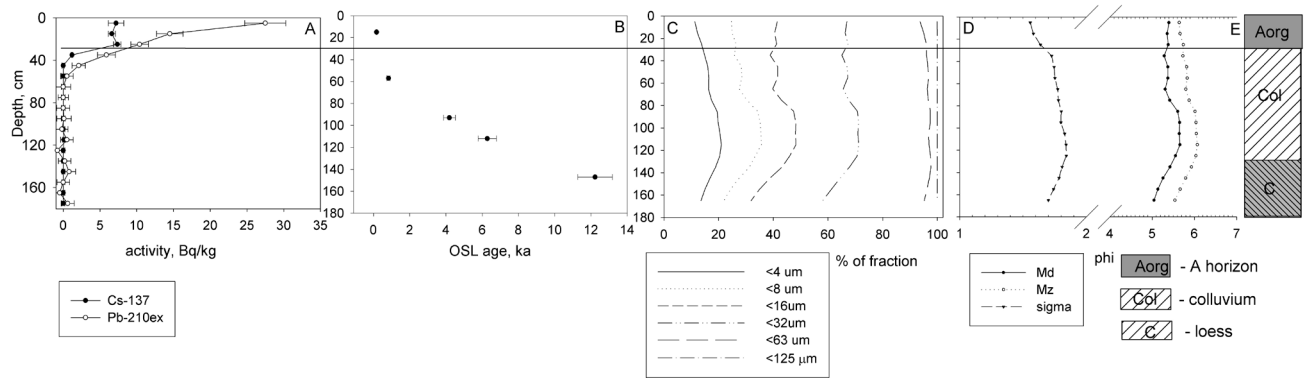
quartz grains into a ploughed A-horizon, **Fig. 14**) (Bateman *et al.*, 2003). Due to pedoturbation (both biological and mechanical mixing) a part of quartz grains move up to the topographic surface where the luminescence signal may be bleached. Just before the sediment transport on the slope, or at the beginning of this process, more than 90% of the initial luminescence signal is bleached. Similar results have been obtained for sandy loess in the south of Poland (Poręba *et al.*, 2015). In the case of sampling points located at the base of the slope, 5 sediment samples were OSL dated (**Fig. 12**). All OSL ages are consistent with a stratigraphic order. The age of the sediment sample from the top soil is equal to 0.175 ka (Bie_4_1; GdTL-3071). Below, very close to the surface, the age of the sediment sample equals 0.838 ka (Bie_4_2; GdTL-3072). The next part of the sediment core is represented by two luminescence results within the range 4.20–6.28 ka (Bie_4_3 and Bie_4_4; GdTL-3073, GdTL-3074). The younger results are probably due to bioturbation before covering by the next sedimentation. The result of OSL dating of the lowermost sample is equal to 12.28 ka (Bie_4_5; GdTL-3075). This is significantly younger than the expected age of loess cover formation, which may be the result of bioturbation before covering by Neolithic sediment.

In the case of the gully wall sampling point, 13 sediment samples from different sediment horizons were collected for the luminescence study (**Fig. 13**). The age of the sediment sample from the top soil (modern humus soil-horizon) corresponds with the age of sediments collected on the eroded slope. The whole profile could be divided into three main parts. The upper part of the colluvial sediment is clearly the youngest part of the analysed profile, with four luminescence results within the range 0.645–0.746 ka (Bie_1_1 - Bie_1_4; GdTL-2906, GdTL-2907, GdTL-2908 GdTL-2909; **Table 1**). It can also be seen that all 4 dates are within a very small range. For the OSL samples of the middle part of the sediment profile, the results are within the range of 6.05–0.988 ka (Bie_1_5 – Bie_1_9; GdTl-2910, GdTL2911, GdTL2912,

GdTL2913). The lowest dated samples of this part of sediment are connected with the beginning of Neolithic colluvium accumulation (6.05–5.71 ka). The sediment samples B_1_5-B_1_7 are visibly younger than the expected age. This could be a result of the post-sedimentation pedoturbation processes. The visible fossil soil at the ceiling of the top of this sediment profile could confirm this hypothesis. The results of OLS dating for the lowest part of this sediment profile are within the range from 12.22 ka to 7.30 ka (Bie_1_9 - Bie_1_13; GdTL-2914, GdTL-2915, GdTL-2916, GdTL-2917). Those samples were taken from the Late Pleistocene-early Holocene fossil soil. The lowest sample is from the B horizon of fossil soil, whereas the rest of the sample comes from the A horizon of fossil soil. The results of OSL dating for the humus horizon are visibly younger due to the rejuvenation by pedoturbation during the Holocene. The results of OSL ages for the lower part of the A horizon of the Late Pleistocene – Holocene fossil soil are comparable with the previous results of ^{14}C dating (Śnieszko, 1995).

Results of grain size analysis

The results of particle-size analysis, along with the depth distributions of ^{137}Cs and ^{210}Pb$_{ex}$ and OSL ages for three locations on the slope (top, eroded part and foot of the slope) are presented in **Figs. 10–13**. The studied sediment is characterized by only slight variations in grain-size distributions in the zones where the studied radionuclides (^{137}Cs and ^{210}Pb$_{ex}$) occur. Two profiles presented in **Figs. 10C** and **11C** have similar grain-size distributions. Silt is the dominant fraction varying between 77 and 80% and fine silt is the larger subfraction and increases relatively to coarse silt at the base of the solum.

The clay content (<4 μm) is constant and fluctuates between 13.0 and 15.5%. Sand (>63 μm) content also varies little and is less than 10% of the total sediment. The sediments are very poorly sorted (1.56–1.8 φ) and the mean grain size (Mz) varies little (5.04–5.6 φ). The profile presented in **Fig. 12C** shows an increasing clay frac-

Fig. 13. *The results of OSL SAR dating for the side of the gully (B), results of U-238, Th-232 (C) and K-40 (D) analysis as well as grain size analysis (E, F) in samples from the wall of gully. On the figure also shown the results of activity measurements by portable gamma spectrometer (B) and stratigraphy (A).*
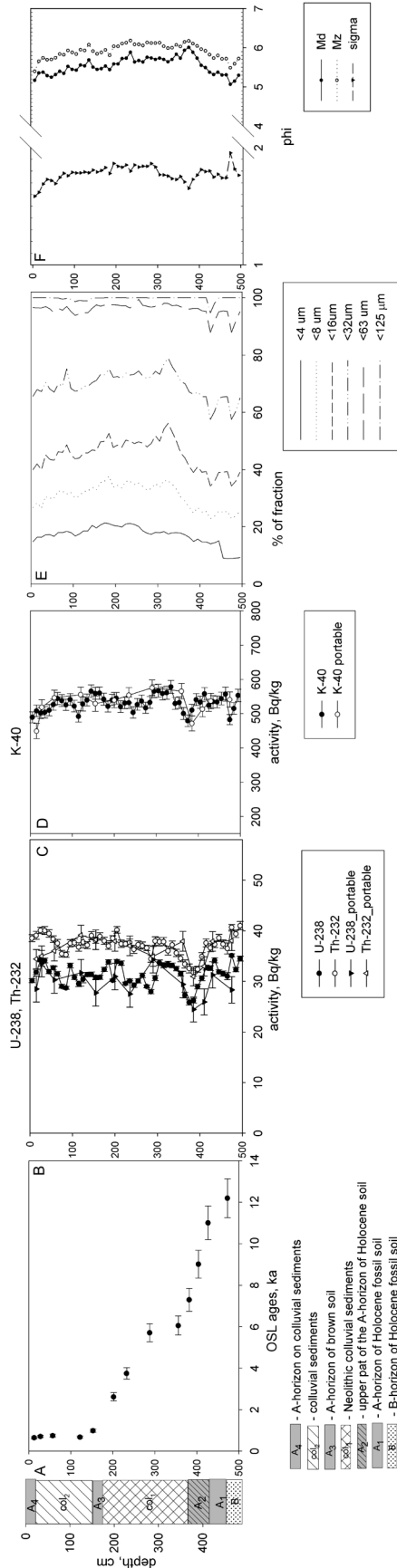
tion with depth through the colluvial sediment. Below the colluvial layer, Mz decreases slightly (**Fig. 12D**).

The sequence presented in **Fig. 13E** has a particle-size distribution which reflects the lithogenic and pedogenic character of particular layers. Shifts between neighbouring units are visible, as is the base of the solum. Clay content is very high (9.5–21.3%) in the middle layer (older colluvium) and lo wer in the lower part of the oldest soil. Maximum clay content is in the Bt horizon of the lower unit, and the minimum is in the uppermost A horizon (10%) and the lower part of the lower colluvial layer. The biggest fluctuations in particle size distribution are recorded in clay and sand content (9.5–21.3% and 0.5–12.0%, respectively). The whole sequence is poorly sorted (δ = 1.6–1.9 ϕ), mean grain size (Mz) varies between 5.0 and 6.0 ϕ (15–29 μm) and average grain size is 21 μm (**Fig. 13F**).

Micromorphology

Typical micromorphological features (**Table 2**, **Fig. 5**) of the lowest soil unit (depth 380–475 cm) are: channel microstructure (common in the whole sequence), clay microfeatures and Fe-Mn nodules (especially common in the middle part). Additionally, the upper part is rich in faecal pellets and pieces of charcoal. Microscopic observations of thin sections showed a "typical" record of occurrence of pedogenic microforms. The clay coatings, infilling recorded inside the channels and fissures are the effect of illuviation processes and the formation of well-developed Bt-argic horizons. The other microfeatures mentioned are also typical pedogenic features, confirming a high level of soil development – Fe-Mn nodules are redoximorphic features; while charcoal pieces – pedogen-

Table 2. *Micromorphology of colluvial-soil sequence at Biedrzykowice. Microstructure: ch – channel, co – coprolithic, ma – massive. Frequency of occurrence: 0 – none, 1 – single, 2 – few, 3 – common, 4 – very common.*

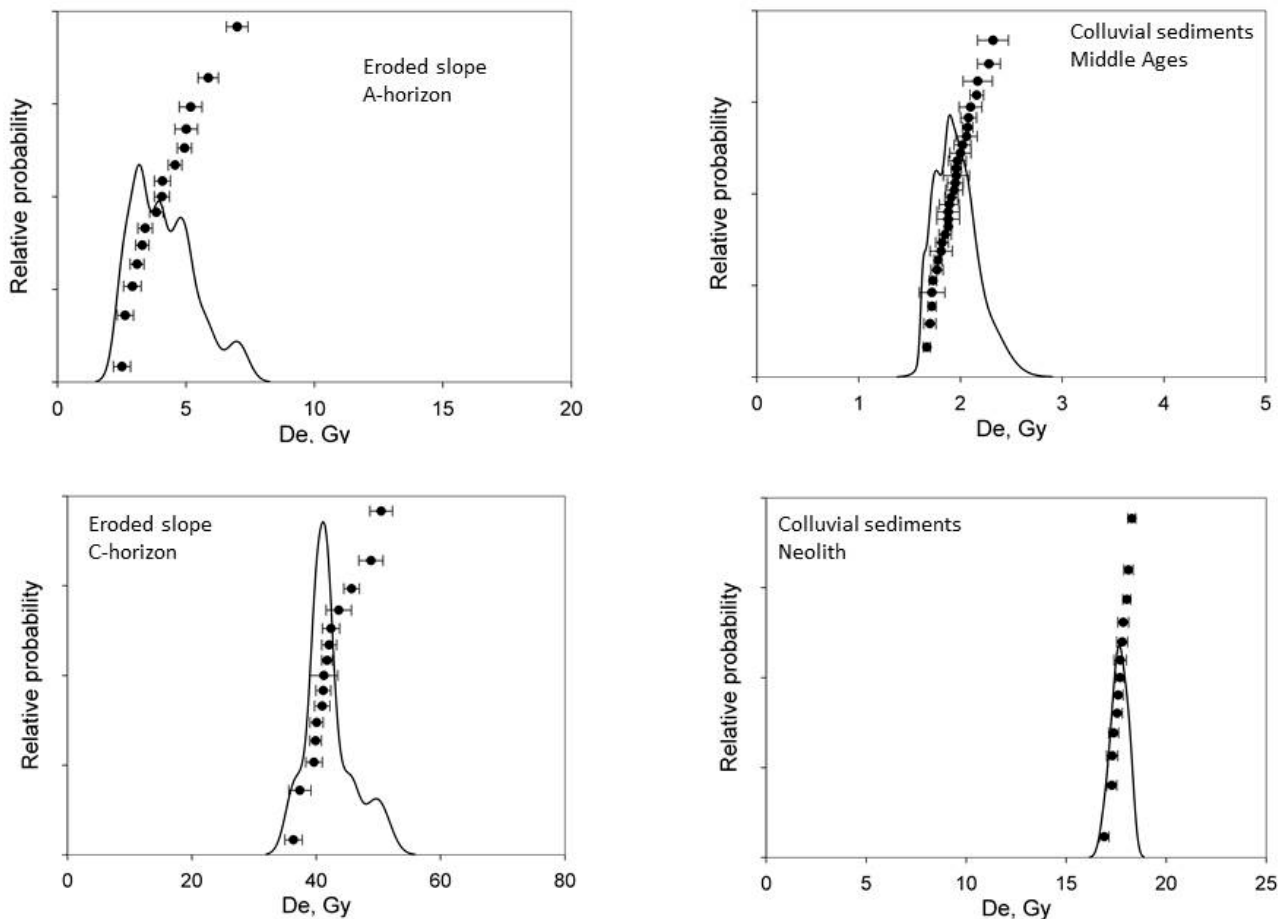| Unit	Depth (cm)	Microstructures	Clay coatings and infillings	Fe and Fe-Mn microforms	Fecal pellets	Charcoals
I	10–15	ch-co	0	0	3	2
	25–30	ch	0	2	2	2
	55–60	ch	1	2	1	0
	120–124	ch	2	2	3	2
II	151–155	ch	2	2	2	2
	200–205	ch	2	2	2	1
	231–235	ch	1	2	2	0
	285–290	ch	0	3	2	0
	355–360	ch	0	3	2	0
III	380–385	ch	0	3	4	1
	405–410	ch	3	2	2	3
	425–430	ch-ma	4	3	2	2
	470–475	ch-ma	2	1	0	0

Fig. 14. *The examples of D_e distributions.*

ic ones. According to palaepedological criteria for the area of the Southern Polish Loess Upland, this type of palaeosol can be described as a buried mature soil developed at the end of the Late Glacial and Early Holocene (e.g. Jersak *et al.*, 1992; Konecka-Betley, 2002).

The middle unit (151–360 cm; **Table 2**; **Fig. 4**) has very similar micromorphological characteristics, but the distribution of diagnostic features is very specific. In the thin sections, all the features mentioned above were also identified. The Fe-Mn microfeatures and fecal pellets were recorded in the whole unit as common and very common forms. The unit is clear ly two-parted, with a division according to the presence of charcoal and clay microfeatures. The upper part is rich in illuvial microforms and also in – but less common – charcoal. Angular clay concentrations are very specific – their distribution is not associated with commonly present biogenic channels. Chaotically arranged clay particles are frequently present inside the groundmass. The micromorphological characteristics suggest this unit is a colluvial soil developed on

older, redeposited soil material. The presence of clay features testifies to the parent material of this soil coming from a redeposited Bt soil horizon.

The main microfeatures of the upper unit (0–124 cm; **Table 2**) correspond with those of the middle unit, but their degree of development is much weaker. The top horizon clearly has pedogenic features – modern faecal pellets and charcoals are common. There are no traces of illuviation and redoximorphic features. The middle and especially lower units have clay and Fe-Mn features (single to common) and faecal pellets (common). The unique features are clay coatings – thin and continuous on the walls of channels. This set of micromorphological features testifies to young pedogenic processes. The lack of older, redeposited clay microforms indicates that the parent material was not directly connected with the older and well developed Bt soil horizon. According to our results of micromorphology analysis, it cannot be excluded that the redeposited material of upper soil horizons of Holocene soil was the parent material of the young soil.

Dendrochronology

Below, the results of dendrochronological analyses are presented for samples taken from trees growing at the base of the slope near the edge of the gully.

Tree no. 1

The tree is tilted perpendicularly to the gully axis, about 75% of its root system is exposed. The distance between the furthest exposed root and the hillslope edge is 1.5 m. The tree we sampled has grown since at least 1938. It was not possible to determine eccentricity because it was not possible to sample a core from the side of the tree exposed to the gully. Strong ring reductions were found in 1970–1978, 1986–1989, 2010–2013 (**Fig. 15A**).

Tree no. 2

The tree is tilted perpendicularly to the gully axis, about 25% of its root system is exposed. The distance between the furthest exposed root and the hillslope edge is 0.5 m. The tree we sampled has grown since at least 1960. Eccentric growth of the tree started in the following years: 1977, 1981, 1996, 1999, 2000, and 2014. Strong ring reductions were found in 1970–1978, 1986–1989, 2010–2013.

Tree no. 3

The tree is tilted perpendicularly to the gully axis, about 50% of its root system is exposed. The distance between the furthest exposed root and the hillslope edge is 0.9 m. The tree we sampled has grown since at least
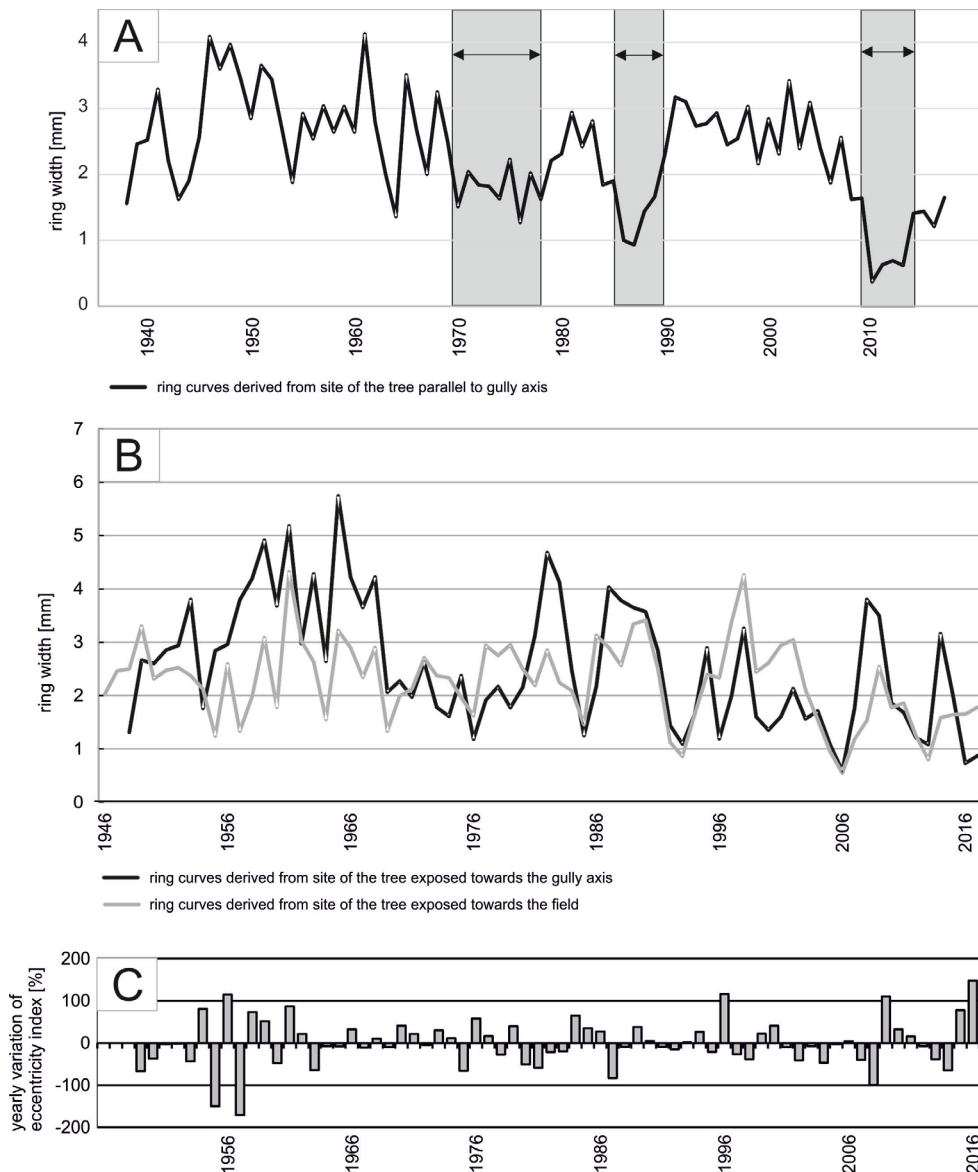

Fig. 15. *Graphs showing strong ring reductions in tree no. 1 signed by arrows and grey surfaces (A), tree ring curves form opposite site of the tree no. 3 (B), and yearly variation of eccentricity index of the tree no. 3 (C)*

1949. Eccentric growth of the tree started in the following years: 1978, 1979, 1983, 1984, 1996, 1998, 1999, 2002, 2010, 1015, 2016. Strong ring reductions were found in 1961–1963, 1968–1973, 1989–1994, 2005–2011 (**Figs. 15B**, **15C**).

Tree no. 4

The tree is tilted perpendicularly to the gully axis, about 50% of its root system is exposed. The distance between the furthest exposed root and the hillslope edge is 0.6 m. The tree we sampled has grown since at least 1953. Eccentric growth of the tree started in the following years: 1957, 1963, 1975, 1976, 1981, 1987, 1996, 2008, 2014, 2016. Strong ring reductions were found in 1970–1976, 1968–1973, 1998–2002, 2010–2017.

Tree no. 5

The tree is tilted perpendicularly to the gully axis, no roots were exposed, tree growing at the distance of 1 m to the gully hillslope edge. The tree we sampled has grown since at least 1949. Eccentric growth of the tree started in the following years: 1957, 1963, 1975, 1976, 1981, 1987, 1996, 2008, 2014, 2016. No strong reductions were found.

Tree no. 6

The tree is tilted perpendicularly to the gully axis, about 50% of its root system is exposed. The distance between the furthest exposed root and the hillslope edge is 1 m. The tree we sampled has grown since at least 1948. Eccentric growth of the tree started in the following years: 1961, 1963, 1971, 1973, 1978, 1980, 1986, 1988, 1993, 1996, 1999, 2002, 2014, 2016. Strong ring reductions were found in 1983–1998, 2010–2015. Additionally from this site, the exposed roots of the studied tree were collected. Roots were exposed: no. 1 – 1993, no. 2 – 1998, no. 3 – 2008, no. 4 – 2014.

4. DISCUSSION

The calculated sedimentation rate for modern soil erosion, based on the ^{137}Cs and ^{210}Pb$_{ex}$ measurements, ranges from almost 0 to 4.5 mm·a^{-1}. The calculated total thickness of soil eroded obtained by the ^{137}Cs and ^{210}Pb$_{ex}$ measurements is quite similar and ranges from 0.3 to 23 cm and from 0.1 to 22 cm, respectively. In the case of sediment accumulation, the calculated total thickness of the accumulated sediments ranges from 4 to 46 cm in the case of the ^{137}Cs measurement and from 1 to 33 cm in the ^{210}Pb$_{ex}$ measurements. The apparent similarity of the results obtained with both isotopes is somewhat surprising, taking into account the range in time of both methods. One possible explanation is the possible change in land use that took place after World War II. There are also visible differences in distribution on the surface of the field between the results of soil erosion and sediment

accumulation obtained using the ^{137}Cs and ^{210}Pb$_{ex}$ methods. The ^{210}Pb$_{ex}$ method indicates that the upper parts of the slope are eroded and a more gradual increase in accumulation takes place from more or less half of its length. In the case of ^{137}Cs, the spatial distribution of erosion and accumulation intensity is slightly different. Rather, it remodels the surface of the slope, and the largest accumulation takes place higher than in the ^{210}Pb$_{ex}$ analyses. The eroded material probably does not reach the edge of the gully (former valley bottom) from the change in land use. Additionally, for the upper part of the colluvial sediment samples collected from the wall of the gully, a limited sediment accumulation was observed for the last 50–100 years. Both the isotope depth distributions, as well as the values of isotope inventories, confirmed this hypothesis. For those sampling points, ^{137}Cs as well as ^{210}Pb$_{ex}$ are present only at the top of the modern A-horizon, which confirms that no mechanical mixing has occurred in this location over the last 50–100 years. The depth distribution of both isotopes, together with the inventories of ^{137}Cs and ^{210}Pb$_{ex}$, suggest that limited sediment delivery during the last 100 years occurred to the site at the edge of the gully. This delivery was probably before the fallout of ^{137}Cs which occurred after the Chernobyl accident. Samples B_1_1 to B_1_4 (gully wall) were dated by the OSL method as medieval colluvial sediment (**Table 1**). At the depth from 150 cm to 365 cm, there is a layer of Neolithic colluvial sediment with visible pedologic features, which was already present by the end of sediment accumulation. Below the Neolithic colluvial sediment are the A and Bt horizons of the Late Vistulian-Early Holocene fossil soil. The OSL dating results of this fossil soil are smaller than the time of its formation. This is due to the rejuvenation of this upper layer of fossil soil before its covering by Neolithic settlements. The situation is similar in the case of Neolithic colluvia, where the upper layer is also rejuvenated. The bleaching process of the OSL signal probably occurred from the end of Neolithic sedimentation to the cover of medieval settlements. The obtained results of micromorphological analyses also seem to confirm this conclusion

For the sediment core located at the foot of the slope, the OSL age of the sediment is 0.175 ka. Although this layer contains ^{137}Cs activity, its depth distribution and inventory suggest no sediment delivery for at least 60 years. The ^{137}Cs and ^{210}Pb$_{ex}$ inventories also confirm the lack of modern sediment. Thus, this OSL age result seems to be reliable. For samples from the deeper layers, the OSL ages correspond to the ages of samples collected from the gully wall. Gully erosion and surface erosion after the deforestation of dry valleys took place simultaneously. The formation of a gully means that agrotechnical treatments on the slopes of the dry valley in which the gully has formed no longer reach its edge. If the area of a gully and its periphery is re-forested, the flow of material eroded away from the farmed slope of the dry

valley to the edge of the gully ceases. Hence, in the Holocene water erosion soil profile that was exposed in the gully wall, no record of sediment caused by erosion of the dry valley slope used for agriculture has been found since the time of afforestation of the gully began.

The medieval colluvial sediment is about 150 cm thick, while the thickness of the Neolithic colluvial sediment is about 180 cm. Unfortunately, there are difficulties in precisely establishing the age of the latest Neolithic colluvial sediment due to pedoturbation. In the case of medieval sediments, the upper layer might have been rejuvenated as well, however, it is significantly less pronounced than in the case of the Neolithic colluvial sediment. While 50 cm of sediment has accumulated over the last 50 years, only about 180 cm of sediment accumulated during the few hundred years of the Neolithic. Thus, in the case of medieval sediment, it can be concluded that the layer of about 150cm thickness accumulated in a very short time. The relatively small age range of medieval sediment suggests that the intensity of erosion at that time exceeded even what we are seeing nowadays. Similar results indicating an increase in medieval erosion have been noted by Fuchs *et al.* (2011). Most probably, the present gully developed quite rapidly as a result of increased runoff and developing furrow erosion. It is worth noting that the Biedrzykowice settlement was probably founded in the 14th century. The first mention was around 1389 A.D.; however, farmed terrain could have started earlier. The first menti on of Działoszyce (4 km from Biedrzykowice) is about 950 A.D. (Schmidt and Heinrich, 2011). It seems, however, that the start of re-using the area was not the reason for such intense erosion. It could have been connected with increased rainfall in the fourteenth century. The catastrophic rainfall in this period and increased erosion in Europe were mentioned by Dotterweich and Dreibrodt (2011). Dotterweich (2003) concluded that the intensity of rainfall in the 14th century was unusually large, which in combination with the change in land use could be the reason for the great intensification of erosion processes in the 14th century.

This resulted in the abandonment of this area as farmland, an invasion by woody vegetation, and consequently in the stoppage/minimization of erosion on the slope. Erosion processes re-started about 50–60 years ago, as indicated by the ^{137}Cs and ^{210}Pb$_{ex}$ isotope measurements, probably due to land use change. The oldest sampled tree, one of the biggest in the studied gully started growing in the 1930's. This indicates the period when in the gully began to grow trees. **Fig. 16** presents the results of dendrochronological dating. We found over a dozen episodes when the hillslope of the gully retreated in the last 50 years, which indicates significant recent changes in gully morphology. Some of the events dated dendrochronologically correspond with large or numerous rainfall events recorded during individual years in the Sielec precipitation gauge located 12 km from the sampling site (1961, 1963, 1970, 1980, 1986, 1996, 1998, 2001, 2010).

Dendrochronological data show more erosion episodes recorded in the last 20 years, but it doesn't mean that erosion has intensified recently. It is more likely that trees have been closer and closer to the hillslope wall, and are more sensitive (their stems could be easily tilted when the root systems were exposed) to the following erosion events.

Long-term research on the Neolithic settlement in Bronocice, and its immediate surroundings in the vicinity of the specific site investigated by the authors, commenced in 1981. Studies on Holocene sediments in river valleys and dry valleys started shortly thereafter and the joint results of archaeological and geological research were published in 1996 (Kruk *et al.*, 1996). At the time, the authors came to the conclusion that there had been an intensification of slope processes in the 5–4 ka BP period on the basis of many indirect premises. There was no direct evidence that could be provided by, for example, radioisotopic dating of slope sediments corresponding to periods of increased anthropogenic soil erosion. The results obtained now by the authors of the present paper finally prove, fully and reliably, the previously formulated theses and allow any prior reservations raised due to the uncertainty of relative dating to be rejected.

The intensification of agricultural colonization in the studied area in the Middle Ages, now confirmed in radiometric dating, has been documented historically as well (Śnieszko, 1985). As in the case of research on the Neolithic colluvium, prior to these measurements there was similarly no direct indisputable evidence of the presence of medieval colluvial sediments corresponding to agricultural land use.

Radiometric measurements of the sediments in Biedrzykowice also confirm another well-established hypothesis in the studies of local pre-history: that of significantly decreased agricultural pressure in the Bronze Age and in the period of Roman influence, as settlements were dispersed and agriculture poorly advanced during that time.

5. CONCLUSIONS

Colluvial sediment dating and erosion rate calculations based on radionuclide analysis were used to perform a detailed study of the Holocene sediment budget of a slope in a loess area in Poland. As shown by the analysis, the area has been contaminated by Chernobyl ^{137}Cs fallout – although this contamination is not strong, the SMBM model is not reliable in this case. The IMBM model, although more complicated, seems a much better choice for the study area. Similar results were obtained using the proportional model. The results of soil erosion obtained with the ^{210}Pb isotope measurement method are smaller and have different spatial variability. This probably reflects the changing agricultural use after World War II.

Modern soil erosion based on results from the ^{137}Cs method is 2.1 kg·m^{-2}·a^{-1}, whereas that obtained by the
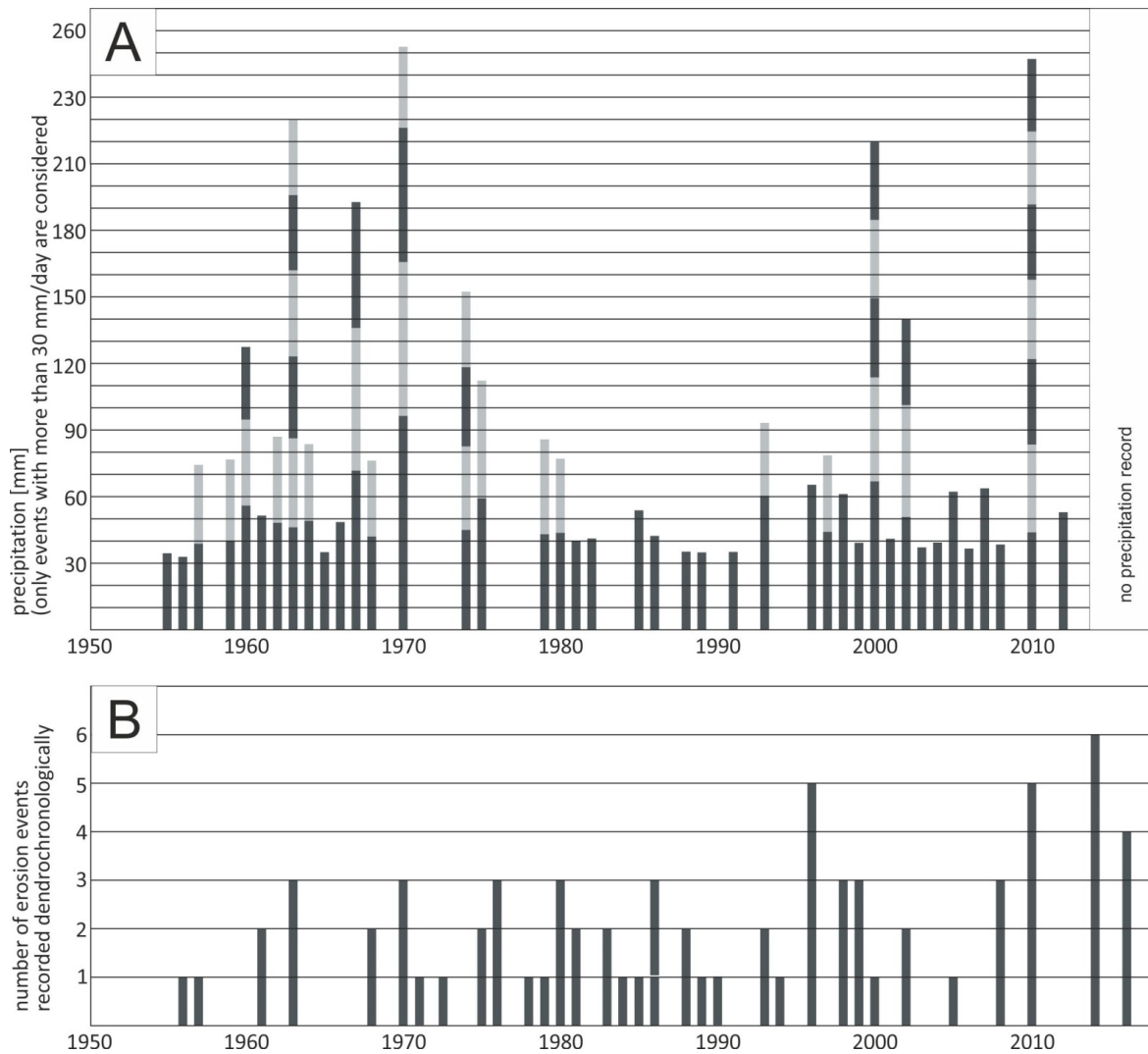
Fig. 16. *Erosion events dated dendrochronologically (B) compared with rainfalls events recorded in Sielec gauge, dark and light grey colour were used one after the other to make more visible the individual rainfall events on the graph (A).*

[210]Pb$_{ex}$ method equals 1.4 kg·m^{-2}·a^{-1}. The rate of erosion on the slope is quite variable. About 100% of the eroded soil has accumulated at the base of the slope. The mean thickness of modern sediment is 30 cm, the thickness of medieval sediment is about 155 cm, with Neolithic sediment about 180 cm thick. Sedimentation rates for the Neolithic sequences compared to those of the medieval periods are lower. The results suggest that the increased intensity of water soil erosion on the sl opes was one of the results of human impact on the environment. The start of sediment accumulation is correlated with the beginning of Neolithic farming. Although the thickness of medieval sediment is less than that of Neolithic sediment, the intensity of soil erosion was probably highest shortly after the reintroduction of farming in the Middle Ages, when gully formation had already started. The current intensity of soil erosion is probably lower than in the past and equals a few cm (up to 23 cm) for the last 50 years. The pattern of soil erosion on the slope suggests that we are currently witnessing slope sediment water transport with redeposition still on the slope.

The precise dating of colluvial sediment suggests that the sedimentation rate and thus also the erosion intensity for the Middle Ages was probably higher than nowadays. The OSL dating results show that colluvial sediments could indeed be dated by this method with sufficient precision, despite the rather short transport of quartz grains on the slope - mainly because the bleaching of the OSL signal begins even before the transport of grains on the slope, and finishes after burial by the next sediment layer at the accumulation site. Simultaneous use of the OSL dating method, the ^{137}Cs and [210]Pb$_{ex}$ isotopic methods and of detailed pedological analysis allowed us to establish a reliable sediment chronology and reconstruct the history of soil erosion and sediment accumulation.

Gully erosion and surface erosion after the deforestation of dry valleys take place simultaneously. The formation of a gully means that agrotechnical treatments on the slopes of the dry valley in which the gorge has formed no longer reach its edge. If the area of a gully and its periphery is re-forested, the flow of material eroded away from the farmed slope of the dry valley to the edge of the gully ceases. Hence, in the Holocene water erosion soil profile that was exposed in the gully wall, no record of sediment caused by erosion of the dry valley slope used for agriculture has been found since afforestation of the gully began.

REFERENCES

Adamiec G and Aitken MJ, 1998. Dose-rate conversion factors: update. *Ancient TL* 16: 37–50.

Aitken MJ, 1985. *Thermoluminescence Dating*. London. Academic Press, 359 pp.

Aitken MJ, 1998. *An introduction to optical dating*. Oxford. Oxford University Press: 267 pp.

Baskaran M, 2011. Po-210 and Pb-210 as atmospheric tracers and global atmospheric Pb-210 fallout: a review. *Journal of Environmental Radioactivity* 102: 500–513, DOI 10.1016/j.jenvrad.2010.10.007.

Bateman MD, Frederick CD, Jaiswal MK and Singhvi AK, 2003. Investigations into the potential effects of pedoturbation on luminescence dating. *Quaternary Science Reviews* 22: 1169–1176, DOI 10.1016/S0277-3791(03)00019-2.

Bluszcz A, 2000. Datowanie luminescencyjne osadów czwartorzędowych – teoria, ograniczenia, problemy interpretacyjne. *Geochronometria* 17, 104 pp. (in Polish, with English summary).

Bodoque JM, Díez-Herrero A, Martín-Duque JF, Rubiales JM, Godfrey A, Pedraza J, Carrasco RM and Sanz MA, 2005. Sheet erosion rates determined by using dendrogeomorphological analysis of exposed tree roots: two examples from Central Spain. *Catena* 64: 81–102, DOI 10.1016/j.catena.2005.08.002.

Bortolot VJ, 2000. A new modular high capacity OSL reader system. *Radiation Measurements* 32: 751–757, DOI 10.1016/S1350-4487(00)00038-X.

Cutshall NH, Larsen IL and Olsen CR, 1983. Direct analysis of 210Pb in sediment samples: self-absorption corrections. *Nuclear Instruments and Methods in Physics Research* 206: 309–312, DOI 10.1016/0167-5087(83)91273-5.

Dotterweich M, 2003. Land Use and Soil Erosion in northern Bavaria during the last 5000 Years. (In:) Lang A, Hennrich K, and. Dikau R (Eds.):, LNES, Springer-Verlag, 101: 201–229.

Dotterweich M, 2008. The history of soil erosion and fluvial deposits in small catchments of central Europe: Deciphering the long-term interaction between humans and the environment — A review. *Geomorphology* 101: 192–208, DOI 10.1016/j.geomorph.2008.05.023.

Dotterweich M and Dreibrodt S, 2011. Past land use and soil erosion processes in central Europe. *Pages news* 2: 49–51.

Dubois G and Bossew P, 2003. Chernobyl 137Cs deposition in Austria: analysis of the spatial correlation of the deposition levels. *Journal of Environmental Radioactivity* 65: 29–45, DOI 10.1016/S0265-931X(02)00062-0.

Fuchs M, Lang A and Wagner GA, 2004. The history of Holocene soil erosion in the Phlious Basin, NE Peloponnese, Greece, based on optical dating. *The Holocene* 14: 334–345, DOI 10.1191/0959683604hl710rp.

Fuchs M and Lang A, 2009. Luminescence dating of hillslope deposits – A review. *Geomorphology* 109: 17–26, DOI 10.1016/j.geomorph.2008.08.025.

Fuchs M, Will M, Kunert E, Kreutzer S, Fischer M and Reverman R, 2011. The temporal and spatial quantification of Holocene sediment dynamics in a meso-scale catchment in northern Bavaria, Germany. *The Holocene* 21: 1093–1104, DOI 10.1177/0959683611400459.

Galbraith RF, Roberts RG, Laslett GM, Yoshida H and Olley JM, 1999. Optical dating of single and multiple grains of quartz from Jinmium rock shelter, Northern Australia: part 1, experimental design and statistical models. *Archaeometry* 41: 339–364, DOI 10.1111/j.1475-4754.1999.tb00987.x.

Gärtner HW, Schweingruber FH and Dikau R, 2001. Determination of erosion rates by analyzing structural changes in the growth pattern of exposed roots. *Dendrochronologia* 19: 81–91.

Golosov V, Walling DE, Panin AV, Stukin ED, Kvasnikowa EV and Ivanova NN, 1999. The spatial variability of Chernobyl-derived 137Cs inventories in a small agricultural drainage basin in central Russia. *Applied Radiation and Isotopes* 51: 341–352, DOI 10.1016/S0969-8043(99)00050-0.

Guerin G, Mercier N and Adamiec G, 2011. Dose-rate conversion factors update. *Ancient TL* 29: 5–8.

He Q and Walling DE, 1996. Interpreting particle size effects in the adsorption of 137Cs and unsupported 210Pb by mineral soils and sediments. *Journal of Environmental Radioactivity* 30: 117–137, DOI 10.1016/0265-931X(96)89275-7.

He Q and Walling DE, 1997. The distribution of fallout 137Cs and 210Pb in undisturbed and cultivated soils. *Applied Radiation and Isotopes* 48: 677–690, DOI 10.1016/S0969-8043(96)00302-8.

Herr AJ, Adamiec G and Moska P, 2012. How many grains are there on a single aliquot? *Ancient TL* 30(1): 9–16.

Isajenko K, Fujak M and Piotrowska B, 2014. Monitoring skażenia 137Cs w glebie w latach 2012–2013. (Monitoring of Cs-137 concentration in soil in 2012-2013). Centralne Laboratorium Ochrony Radiologicznej Zakład Dozymetrii Warszawa (in Polish).

Jary Z, 2007. Record of Climate Changes in Upper Pleistocene loess-soil sequences in Poland and western part of Ukraine). Rozprawy Naukowe Instytutu Geografii i Rozwoju Regionalnego Uniwersytetu Wrocławskiego 1, Wroclaw (in Polish, with English abstract).

Jersak J, 1973. Lithology and stratigraphy of the loess on the southern Polish Uplands. *Acta Geographica Lodziensia* 32: 1–139.

Jersak J, Sendobry K and Śnieszko Z, 1992. Postwarciańska ewolucja wyżyn lessowych w Polsce. (Post-Wartanian evolution of loess upland in Poland). Wyd. UŚ, Katowice 1227, 196 pp. (in Polish).

Kato H, Onda Y and Tanaka Y, 2010. Using 137Cs and 210Pbex measurements to estimate soil redistribution rates on semi-arid grassland in Mongolia. *Geomorphology* 114: 508–519, DOI 10.1016/j.geomorph.2009.08.009.

Kemp R, 2001. Pedogenic modification of loess: significance for palaeoclimatic reconstructions. *Earth-Science Reviews* 54: 145–156, DOI 10.1016/S0012-8252(01)00045-9.

Kondracki J, 2002. Geografia regionalna Polski. (Regional geography of Poland). PWN, Warszawa. (in Polish).

Konecka-Betley K, 2002. Paleosols of different age developed from loess in Poland. In: B. Manikowska K, Konecka-Betley K, Bednarek R, (eds.), Problemy paleopedologii w Polsce, TN, Łódź: 135–163.

Kruk J, Milisauskas S, Alexandrowicz SW and Śnieszko Z, 1996. Osadnictwo i zmiany środowiska naturalnego wyżyn lessowych, (Environmental Changes and settlement on the loess Uplands. An

archaeological and palaeogeographical study on the Neolithic In the Nidzica bassin (Summary). Kraków (Instytut Archeologii i Etnologii PAN). pp: 7–139 (in Polish).

Kruk J and Milisauskas S, 1999. Rozkwit i upadek społeczeństw rolniczych neolitu. The Rise and Fall of NeolithicSocietes. Kraków. Instytut Archeologii i Etnologii Polskiej Akademii Nauk. (in Polish).

Kruk J, Lityńska-Zając M and Milisauskas S, 2016. Gospodarka roślinna w neolicie. Studium przypadku – Bronocice. (Neolithic Plant Cultivation at Bronocice). IAiE PAN, 224 pp. (in Polish).

Lang A, 2003. Age and source of colluvial sediments at Vaihingen-Enz, Germany. *Catena* 38: 89–107, DOI 10.1016/S0341-8162(99)00068-5.

Lee J and Kemp RA, 1992. Thin section of unconsolidated sediments and soils. a recipe, Thin Section Laboratory, Sediment Analysis Suite, Geography Department, Royal Holloway, University of London, Egham: 1–32.

Lu XX and Higgitt DL, 2000. Estimating erosion rates on sloping agricultural land in the Yangtze Three Gorges, China, from caesium-137 measurements. *Catena* 39: 33–51, DOI 10.1016/S0341-8162(99)00081-8.

Li M, Li Z, Yao W and Liu P, 2009. Estimating the erosion and deposition in a small watershed by the ^{137}Cs tracing method. *Applied Radiation and Isotopes* 67: 362–366, DOI 10.1016/j.apradiso.2008.10.011.

Mabit L, Benmansour M and Walling DE, 2008. Comparative advantages and limitations of the fallout radionuclides ^{137}Cs, [210]Pb$_{ex}$ and [7]Be for assessing soil erosion and sedimentation. *Journal of Environmental Radioactivity* 99: 1799–1807, DOI 10.1016/j.jenvrad.2008.08.009.

Mabit L, Benmansour M, Abril JM, Walling DE,Meusburger K, Iurian AR, Bernard C, Tarjan S, Owens PN, Blake WH and Alewell C, 2014. Fallout ^{210}Pb as a soil and sediment tracer in catchment sediment budget investigations: A review. *Eart-Science Reviews* 138: 335–351, DOI 10.1016/j.earscirev.2014.06.007.

Malik I, 2006a. Contribution to understanding the historical evolution of meandering rivers using dendrochronological methods: example of the Mała Panew River in southern Poland. *Earth Surface Processes and Landforms* 31: 1227–1245, DOI 10.1002/esp.1331.

Malik I, 2006b. Gully erosion dating by means of anatomical changes in exposed roots (Proboszczowicka Plateau, Southern Poland). *Geochronometria* 25: 57–66.

Malik I, 2008. Dating of small gully formation and establishing erosion rates in old gullies under forest by means of anatomical changes in exposed tree roots (southern Poland). *Geomorphology* 93: 421–436, DOI 10.1016/j.geomorph.2007.03.007.

Malik I and Wistuba M, 2012. Dendrochronological methods for reconstructing mass movements — an example of landslide activity analysis using tree-ring eccentricity. *Geochronometria* 39: 180–196, DOI 10.2478/s13386-012-0005-5.

Maruszczak H, 1991. Zróżnicowanie stratygraficzne lessów polskich. (Stratigraphic differentiation of Polish loess). In: H. Maruszczak (Ed.), Podstawowe profile lessów w Polsce. Wyd. UMCS, Lublin: A.13-A.15. (in Polish).

Maruszczak H, 2001. Schemat stratygrafii lessów i gleb śródlessowych w Polsce. (Scheme of loesses and intra-loess soils in Poland). In: H. Maruszczak (ed.), Podstawowe profile lessów w Polsce II. Wyd. UMCS, Lublin: 17–29. (in Polish).

Mason JA, Jacobs PM and Greene RSB, 2003. Sedimentary aggregates in the Peoria Loess of Nebraska, USA. *Catena* 53: 377–397, DOI 10.1016/S0341-8162(03)00073-0.

Moska P, Poręba G and Bluszcz A, 2004. The influence of cesium activity on the annual dose for OSL dating. *Geochronometria* 23: 15–19.

Mroczek P, 2008. Interpretacja paleogeograficzna cech mikromorfologicznych neoplejstoceńskich sekwencji lessowo-glebowych (Palaeogeographic interperation of micromorphological features of Neopleistocene loess–palaeosol sequences). Maria Curie Skłodowska University Press, Lublin, 130 pp. (in Polish, with English summary).

Mroczek P, 2013. Recycled loesses – a micromorphological approach to determination of local source areas of Weichselian loess. *Quater-*

nary *International* 296: 241–250, DOI 10.1016/j.quaint.2013.02.040.

Mroczek P, 2018. Późnovistuliańsko-holoceńska ewolucja lessowych gleb płowych wyżyn południowopolskich w świetle badań mikromorfologicznych. (Late Vistulian-Holocene Evolution of Loess Luvisols from the South Polish Uplands Recorded in Micromorphology). Wydawnictwo UMCS, Lublin 109 (in Polish with English abstract)

Murray AS and Wintle AG, 2000. Luminescence dating of quartz using an improved single-aliquot regenerative-dose protocol. *Radiation Measurements* 32: 57–73, DOI 10.1016/S1350-4487(99)00253-X.

Paszyński J and Kluge M, 1986. Klimat Niecki Niedziańskiej. (Climate of the Nida Basin). Studia Ośrodka Dokumentacji Fizjograficzej 14: 211–238. (in Polish).

Pietrzak-Flis Z, 2000. Skażenia promieniotwórcze środowiska i człowieka w Polsce. (Radioactive contamination of the environment and human in Poland). *Postępy Fizyki* 51: 70–72. (in Polish).

Poręba G, Moska P and Bluszcz A, 2006. On the contribution of radioactive fallout isotopes to the total dose rate in dating of young sediments. *Geochronometria* 25: 47–50.

Poręba G, 2006. Cesium-137 as a soil erosion tracer – a review. *Geochronometria* 25: 37–46.

Poręba G and Bluszcz A, 2007. Determination of the initial ^{137}Cs fallout on the areas contaminated by Chernobyl fallout. Geochronometria 26: 34–38, DOI 10.2478/v10003-007-0009-y.

Poręba G and Bluszcz A, 2008. Influence of the parameters of models used to calculate soil erosion based on ^{137}Cs tracer. *Geochronometria* 32: 21–27, DOI 10.2478/v10003-008-0026-5.

Poręba G, Śnieszko Z and Moska P, 2015. Application of OSL dating and ^{137}Cs measurements to reconstruct the history of water erosion: A case study of a Holocene colluvium in Świerklany, south Poland. *Quaternary International* 374: 187–197, DOI 10.1016/j.quaint.2015.04.004.

Porto P, Walling DE, Callegari G and Catona F, 2006. Using fallout lead-210 measurements to estimate soil erosion in three small catchments in Southern Italy. *Water, Air, and Soil Pollution* 6: 293–303, DOI 10.1007/s11267-006-9050-5.

Prescott JR and Hutton JT, 1994. Cosmic ray contributions to dose rates for luminescence and ESR dating: large depths and long-term time variations. *Radiation Measurements* 23: 497–500, DOI 10.1016/1350-4487(94)90086-8.

Raven P, Evert R and Eichhorn S, 1999. *Biology of Plants*. W. H. Freeman and Company, New York, 944 pp.

Ritchie J and McHenry JR, 1990. Application of radioactive fallout cesium-137 for measuring soil erosion and sediment accumulation rates and patterns: a review. *Journal of Environmental Quality* 19: 215–233, DOI 10.2134/jeq1990.00472425001900020006x.

Sarmiento JL and Gwinn E, 1986. Strontium 90 fallout prediction. *Journal of Geophysical Research* C6: 7631–7646.

Schweingruber FH, Kontic R, Niederer M, Nippel CA and Winkler-Seifert A, 1985. Diagnosis and distribution of conifer decay in the Swiss Rhone Valley a dendrochronological study. In: H. Turner, W. Tranquillini (Eds.) Establishment and tending of subalpine forest (pp. 189–192). Berno: Swiss Federal Institute of Forestry Research.

Schaetzl R, Forman S and Attig J, 2014. Optical ages on loess derived from outwash surfaces constrain the advance of the Laurentide Ice Sheet out of the Lake Superior Basin, USA. *Quaternary Research* 81: 318–329, DOI 10.1016/j.yqres.2013.12.003.

Schmidt R and Heinrich J, 2011. 200 years of land-use change and gully erosion – a case study from Małopolska, SE Poland. *Landform Analysis* 17: 167–171.

Stoffel M, Casteller A, Luckman BH and Villalba R, 2012. Spatiotemporal analysis of channel wall erosion in ephemeral torrents using tree roots — an example from the Patagonian Andes. *Geology* 40: 247–250, DOI 10.1130/G32751.1.

Stach A, 1996. Możliwości i ograniczenia zastosowania cezu-137 do badań erozji gleb na obszarze Polski. (Possibilities and limitations of Cs-137 application for soil erosion research in Poland) In: Ochrona agroekosystemów zagrożonych erozją. Ogólnopolskie Sympozjum Naukowe, Puławy 1996: 203–226. (in Polish).

Starkel L, 2005. Anthropogenic soil erosion Since the Neolith In Poland. *Zeitschrift fur Geomorphologie* 139: 189–201.

Strzelecki R, Szewczyk J, Wołkowicz S and Jędrzejczak Z, 1992. Badania promieniotwórczości gamma na obszarze Polski: efekt Czarnobyla, skażenia przemysłowe, promieniotwórczość naturalna. (Gamma-radioactivity measurements in Poland: Chernobyl effect, industrial pollution, natural radioactivity). *Przegląd Geologiczny* 6: 365–371. (in Polish).

Strzelecki R, Wołkowicz S and Lewandowski P, 1994. Koncentracje cezu w Polsce. (Concentration of Cesium in Poland). *Przegląd Geologiczny* 1: 3–8 (in Polish).

Sutherland RA, 1992. Caesium-137 estimates of erosion in agricultural areas. *Hydrological Processes* 6: 215–225, DOI 10.1002/hyp.3360060209.

Szewczyk J, 1994. Wpływ skażeń czarnobylskich na poziom promieniowania gamma. (The effect of Chernobyl contamination on the level of gamma radiation) *Przegląd Geologiczny* 6: 450–454 (in Polish).

Śnieszko Z, 1985. Paleogeografia holocenu w dolinie Sancygniówki. (Holocene paleogeography in the Sancygniówka valley) *Acta Geogr.* Lodz. 51 (ŁTN, Łódź.):7–119 (in Polish).

Śnieszko Z, 1987. *The late Vistulian and Holocene fluvial deposits of the middle Nidzica river in the area of Działoszyce*. In: Starkel, L. (ed.), Evolution of the Vistula river valley during the last 15 000 years, part II. Geographical Studies, Special Issue, 4: 87–94.

Śnieszko Z, 1991. *Reflection of extreme events In evolution of dry valleys In loess Roztocze Upland*. In: Less iosadydolinne. Ed J. Jersak. Sosnowiec: 119–129.

Śnieszko Z, 1995. *Ewolucja obszarów lessowych Wyżyn Polskich w czasie ostatnich 15 000 lat. (The loess cover evolution during last 15 000 years in Polish Upplands)*. Wyd. UŚ, Katowice, pp.122. (in Polish, with English summary).

Vandekerckhove L, Muys B, Poesen J, De Weerdt B and Coppé N, 2001. A method for dendrochronological assessment of medium-term gully erosion rates. *Catena* 45: 123–161, DOI 10.1016/S0341-8162(01)00142-4.

Walling DE and Quine TA, 1990. Calibration of caesium137 measurements to provide quantitative erosion rate data. *Land Degradation and Rehabilitation* 2: 161–175.

Walling DE, 1998. Use of ^{137}Cs and other fallout radionuclides in soil erosion investigations: progress, problems and prospects. In: Use of ^{137}Cs in the Study of Soil Erosion and Sedimentation. International Atomic Energy Agency Publication IAEA-TECDOC-1028, pp: 39–64.

Walling DE and He Q, 1999. Improved models for estimating soil erosion rates from cesium-137 measurements. *Journal of Environmental Quality* 28: 611–622, DOI 10.2134/jeq1999.00472425002800020027x.

Wistuba M, Malik I, Gärtner H, Kojs P and Owczarek, 2013. Application of eccentric growth of trees as a tool for landslide analyses (an example of Picea abies Karst. in the Carpathian and Sudeten Mountains – Central Europe). *Catena* 111: 41–55, DOI 10.1016/j.catena.2013.06.027.

Zadorova T, Penizek V, Šefrna L, Drabek O, Mihaljevic M, Volf Š and Chuman T, 2013. Identification of Neolithic to Modern erosion-sedimentation phases using geochemical approach in a loess covered sub-catchment of South Moravia, Czech Republic. *Geoderma* 195: 56–69, DOI 10.1016/j.geoderma.2012.11.012.

Zhang XB, Higgitt DI and Walling DE, 1990. A preliminary assessment of the potential for using caesium-137 to estimate rates of soil erosion in the Loess Plateau of China. *Hydrological Sciences* 35: 243–252.

Zhang XB, Walling DE and He Q, 1999. Simplified mass balance models for assessing soil erosion rates on cultivated land using caesium137 measurements. *Hydrological Sciences* 44: 33–45, DOI 10.1080/02626669909492201.

Zolitschka B, Behr K-B and Schneider J, 2003. Human and climatic impact on the environment as derived from colluvial, fluvial and lacustrine archives – examples from the Bronze Age to the Migration Period, Germany. *Quaternary Science Reviews* 22: 81–100, DOI 10.1016/S0277-3791(02)00182-8.